TORNADO WARNING GUIDANCE

(2nd Edition, Spring 1999)

from the

NATIONAL SEVERE STORMS LABORATORY

and the

WSR-88D OPERATIONAL SUPPORT FACILITY

Points of Contact

Table of Contents

PREFACE

This is the Spring 1999 edition of the Tornado Warning Guidance document. This edition updates the information contained in the previous edition that was developed for the 1997 convective season. Some of the information in the document is unchanged from the 1997 document, but much of it is updated. In particular, a few of the general guidance comments are updated, and a few new comments have been added. A new section is included describing the Build 10 Tornado Detection Algorithm (TDA), and is to be used as a supplement to the Build 10 TDA training manuals. A section was renamed from "Radar Guidance" to "Latest results from NSSL algorithm development (MDA and TDA)". This section describes some statistical analysis of radar algorithm data using NSSL's experimental algorithms (which are available on WATADS). Many new figures and findings are presented in this section. Finally, some of the references have been updated. It is

recommended that all WSR-88D users read this document fully to remain up-to-date on the latest information.

Points of Contact [Top]

The individuals responsible for this document are:

- Greg Stumpf (NSSL), editor and contributor
- Bob Lee (OSF/Applications), contributor
- Caren Marzban (NSSL), contributor
- Erik Rasmussen (NSSL), contributor
- DeWayne Mitchell (NSSL), contributor
- Don Burgess (OSF/OTB), co-editor and contributor
- Mike Magsig (OSF/OTB), contributor
- Brad Grant (OSF/OTB), contributor
- Liz Quoetone (OSF/OTB), contributor
- John Ferree (OSF/OTB), contributor
- Jim LaDue (OSF/OTB), contributor
- Dave Zittel (OSF/Applications), contributor

1. Introduction [Top]

Discriminating between thunderstorms likely to produce a tornado and those not likely to produce a tornado is very difficult. Operational meteorologists tasked with issuing tornado warnings are faced with many challenges. Many inputs, including radar signatures, spotter reports, and the mesoscale environment, play a part in the decision-making process. The most often used WSR-88D signatures in this process are a three-dimensional analysis of the magnitude of mesocyclone rotation in a storm, the strength of gate-to-gate shears, or presence of a Bounded Weak Echo Region (BWER) or hook echo. Many times, radar data has helped generate tornado warnings with significant lead time. However, occasionally tornadoes have occurred without warnings, or warnings based upon rotation have resulted in false alarms. The primary reasons for this are that the radar suffers from sampling limitations, and the tornado formation process is not yet well understood.

The information in this document is meant to provide meteorologists with some of the latest research findings related to the tornado warning decision-making process. This information is based on preliminary research results from the Verification of the Origins of Rotation in Tornadoes EXperiment (VORTEX) (Rasmussen et al. 1994), as well as the statistical analysis of a significant number of WSR-88D storm cases from a variety of sites across the U.S. as part of the mesocyclone and tornado detection algorithm research being performed at NSSL.

Research continues at the National Severe Storms Laboratory (NSSL) and elsewhere to improve the ability to discriminate between tornadic and non-tornadic storms. One of the primary goals of VORTEX *(*which was conducted in Central and Southern Great Plains) was to increase our understanding of why some storms produce tornadoes while others do not. While detailed analysis of the data is ongoing, some observations can be made and considered important guidance for the warning forecaster. A list of tornado warning considerations, including some gathered from analysis of the VORTEX data sets, will be presented in Section 2.

The WSR-88D Build 10 includes the new Tornado Detection Algorithm (TDA) (Mitchell et al. 1998) which has replaced the pre-Build 10 TVS Algorithm (hereafter “old TVS Algorithm”). This software upgrade represents a significant improvement in the way the original algorithm detects tornadic vortex signatures. For example, less stringent strength thresholds are used in the TDA than in the old TVS Algorithm, and a more robust vertical association scheme is used. In addition, the TDA will operate independently of the WSR-88D Mesocyclone Algorithm (88D-MA) and will not require the presence of a mesocyclone detection. Section 3 of this document includes information on the Build 10 TDA to supplement the Build 10 training guides.

NSSL has expended considerable effort to improve the performance of WSR-88D algorithms that are used in the tornado warning decision-making process. The NSSL Mesocyclone Detection Algorithm (MDA) (Stumpf et al. 1998) includes the ability to detect a broader spectrum of storm-scale vortices such as low-topped or mini supercells, and displays the algorithm output with a variety of color-coded tables, ranking attributes, and trend charts. In addition, the NSSL MDA has the capability to provide automated support to forecaster decision-making through the use of neural

network probabilities. The NSSL MDA Algorithm will be a candidate for the first software upgrade after implementation of the WSR-88D Open Systems RPG (ORPG). The NSSL MDA is available right now via the WATADS software for testing on previously-collected WSR-88D data sets. NSSL also continues the experimental development of the TDA. This slightly more robust version of the Build 10 TDA, known as the NSSL TDA, is also available via WATADS. NSSL has also developed a BWER Algorithm which has been undergoing testing since 1998.

Section 4 of this document contains statistics from the NSSL MDA, NSSL TDA, and the NSSL BWER Algorithm on a large data set of tornado-producing storms as well as some non-tornadic supercell events. The location and storm type for the 43 days which comprised the statistical radar guidance data base are given in Table 1. This 43-day data set is larger, by 14 cases, than the data set used to develop the statistics in the 1st Edition of the Tornado Warning Guidance document (Spring 1997). This expanded 43-case data set is more geographically (and synoptically) diverse, and contains eight new "null" cases (no tornadoes reported).

Section 5 summarizes this document. With the delivery of ORPG to the field in two to three years, radar assistance in the detection and warning of tornadoes should be improved. For the near term and even beyond any known improvements, meteorologists are encouraged to continue using **ALL** possible information at their disposal in order to issue successful tornado warnings. This includes spotter reports, storm history, mesoscale environment, and storm/vortex evolution and trends (including reflectivity trends).

2. General Guidance [Top]

This section provides a list of tornado warning guidance that is based on a combination of 1) observations of tornadic storms during VORTEX, 2) applied research utilizing a number of WSR-88D case studies, and 3) observations during operational real-time tests of the NSSL Warning Decision Support System (WDSS). Some of this list was compiled by comments from the VORTEX scientists after the two-year field phase (1994-1995) of the experiment ended. It contains scientists' initial impressions during the field experiment and some preliminary qualitative results regarding tornadogenesis. The list may be updated or refined at a later date as more conclusive quantitative results are formulated and a stronger consensus is reached by scientists involved in various projects.

a) Supercells tend to produce significant tornadoes in regions with enhanced near-ground storm-relative helicity. In many situations, enhanced low-altitude helicity will be associated with backed and strengthened surface winds. All available low-altitude wind data should be monitored, including routine surface observations, mesonetwork data, and lowest-tilt radial velocity. Mesoanalysis is very important. The near-storm environment can vary dramatically over fairly short distances and is subject to rapid change (this was observed on many VORTEX storm days; see Markowski et al. 1998)

b) Because of baroclinic effects along shallow boundaries, the immediate cool side of the boundary is often an area of strongly enhanced horizontal vorticity. Even lacking wind and temperature data, the mere presence of a boundary should lead to heightened awareness, and storms crossing or interacting with boundaries merit special scrutiny for rapid increases in rotation in their lower altitudes. This implies that forecasters need to remain aware of the locations of radar fine lines, satellite-indicated cloud lines, and mesonet-detected surface temperature gradients and wind-shift lines. **Storms interacting with boundaries should be closely monitored because tornadogenesis can occur rapidly.**

c) The chances for significant tornadoes on the cool side of boundaries decrease as low-altitude cold air becomes increasingly deep and CAPE approaches zero. These are difficult to assess in real time, but the key fact is that if the air still contains some CAPE, despite being relatively cool, the potential for significant tornadoes exists; the potential is greatest where the cool air is shallowest and the enhanced helicity resides near the ground (the *immediate* cool side of a boundary, where the temperature difference between the two air masses is still rather small).

d) A high quality spotter network is vital. Whenever possible, one should not rely solely on radar data for making warning decisions, as even storms having strong low-altitude mesocyclones may not produce a tornado (this was observed several times during *VORTEX*). Warning forecasters should make use of all available information including reliable spotter reports (especially when storms are at far ranges), storm history, other remote sensing tools (e.g., satellite), as well as having a good understanding of the mesoscale environment of the storm.

e) Be aware that some storms may produce tornadoes rapidly with little advance warning in the way of algorithm detections or rotation at the 0.5° volume scan. Often, the only low-altitude precursor from radar in these situations is an area of strong, low-altitude (0-2 km AGL) convergence (Burgess and Magsig 1998) below the base of the organizing mesocyclone (remember that 0-2 km AGL information is only observable out to about 65 nm). Also, second and succeeding mesocyclone cores (cyclic mesocyclogenesis) typically have very short organizing stages as they quickly form over a large depth and strengthen rapidly. Therefore, explosive development can take place during the period of a single volume scan. The opposite (rapid dissipation) was also observed during VORTEX.

f) Not every TVS forms at mid altitudes and builds downward over time with the embryonic tornado. Trapp et al. (1998) observed that some TVSs develop rapidly near the surface or simultaneously at low and mid altitudes, especially in squall-lines (but also in some supercells). Be aware of both types of TVS development, and anticipate low-level development with squall lines.

g) Storm motion and tornado motion (direction and speed) may be significantly different. For example, on two VORTEX days (6/2/95 and 6/8/95), there were several instances where the parent thunderstorm was moving toward the northeast while the tornado was moving north. In addition, for another case, the tornado's forward movement was measured at 60 mph only to become nearly stationary before it dissipated. (Learning more about the reasons for changes in tornado motion will be a topic of future VORTEX research). Be careful about issuing tornado warning locations based on the storm cell centroid motions; use the motion of the radar vortex signature, whenever available.

h) In many instances, the radar-observed vortex signature can, depending on range, appear to dissipate **prior to** the actual dissipation of the tornado, as the shrunken tornado vortex (or tornado cyclone) becomes increasingly difficult to observe given WSR-88D sampling limitations. This period without a radar-observable vortex signature **may** include the most intense and damaging phase of the tornado. It is a good rule of thumb to continue tornado warnings for a few volume scans following the dissipation of the radar-observed vortex signature, especially in the absence of reliable spotter information and/or during nighttime hours.

i) Data collected during VORTEX using the Doppler On Wheels (DOW), and data from a variety of WATADS-analyzed WSR-88D cases, verify that a variety of vortex scales occur within storms, ranging from the scale of the actual *tornado* (and even its sub-vortices), up to the scale of the rotating updraft/downdraft of the supercell storm (*mesocyclone*), with vortices intermediate to these scales also occurring (sometimes referred to as the *tornado cyclone*). Some data suggest that these vortices may be embedded within each other, or that some vortices may taper or widen in diameter at different heights. Radar users should be aware that the WSR-88D, with its inherent sampling limitations, may detect a mixture of

these kinds of vortices. Operators should also be aware that only in very rare instances can the WSR-88D actually observe the actual tornado, again, owing to the sampling limitations of the radar (the tornado must be very large and/or very close to the radar). In most instances, a TVS is actually the signature of an intermediate-scale vortex, observed as a gate-to-gate velocity couplet. See this presentation by Stumpf (1998) for figures.

j) Radar-observable vortex signatures which are associated with tornadoes can occur with a variety of storm types. These range from the classic Great Plains supercell (with large horizontal and vertical extent) as well as supercells with small horizontal extent (mini supercells), supercells with small vertical extent (low-topped supercells), or both (low-topped mini supercells). Tornadoes and radar-observable vortex signatures have also been observed with storms embedded within tropical cyclone rain bands ("TC-mesos"), along the leading edge and comma head of bow-echo squall lines, and with rapidly-developing convection (non-supercell tornadoes, landspouts, waterspouts). Do not be misled into believing that all supercells are the same - like the classic big isolated supercells more common to the Central and Southern Plains. Be aware that many varieties exist, including some that probably have not yet been observed. NSSL maintains a WSR-88D tornado case-study Web page that contains the description (with figures) of a number of these typical and atypical tornadic storm cases.

k) Because the WSR-88D provides only discrete horizontal samples of the atmosphere (1° azimuthal resolution; 1 km and 250 m range resolution for reflectivity and velocity respectively), storm-scale vortices can only be depicted in a degraded sense (Wood and Brown 1997). Factors include vortex core diameter to beam width radius ratio, strength of rotation in the vortex, and the offset between the vortex centroid and the centroid of the radar beam. A particular vortex of a given diameter and rotational velocity could be viewed by the radar in a number of configurations given its range from the radar and the vortex/beam centroid offsets. And, if a vortex is shaped asymmetrically, changes in viewing angle will also alter its radar depiction. Consider that these sampling limitations will reduce the velocity estimate of the vortex. Consult Wood and Brown (1997) for information depicting the degree of velocity degradation in radar-sampled vortices.

l) At extended ranges, the radar horizon prevents sampling below the mid-altitudes of mesocyclones. Thus, the radar may observe mid-altitude rotation that is strong for storms at extended ranges, but the radar cannot determine if the low-altitude rotation is strong or even exists. Users should employ the use of spotter reports, or data from another radar sampling the signature from a closer range. At near ranges, the "cone-of-silence" effect will prevent sampling of vortices above a certain altitude, and only a portion of the vortex can be diagnosed for warnings. Forecasters should use data from other WSR-88Ds at farther ranges to sample the mid- and high-altitude data being missed in the cone-of-silence.

m) Many algorithm-detected radar-observable vortex signatures (both mid-altitude and low-altitude) are NOT associated with tornadoes on the ground. Bear in mind that in some

instances, atmospheric vortices can be too small (owing to sampling limitations), or hidden by radar data artifacts (such as range-folded data). Radar algorithms cannot detect these unobservable vortices. Also, some vortex detections may be the result of dealiasing errors, leading to false detections. The user should examine velocity images along with algorithm output at all times.

n) When issuing a warning based on radar, remember the total time involved includes: viewing and analyzing the radar vortex signature (this can take anywhere from 1 minute to 6 minutes if you are using algorithm products as guidance, as they are generated at the **end** of a volume scan), mechanically composing the warning message (2-3 min., or 1 min if using AWIPS), and disseminating the warning (1 min. or more). With the possible lapse of 3 to 10 minutes of time, the location of the mesocyclone or Tornadic Vortex Signature (TVS) that triggered the decision to issue the warning could have moved a considerable distance. Thus, this translated distance of the signature needs to be taken into account when locations are mentioned in the warning (especially when using algorithm overlays for location guidance). This translated distance also needs to be considered for warnings in downstream counties.

o) Adaptable parameter sets are being provided with the Build 10 TDA that correspond to a variety of storm types. It is important to understand that storm types are a factor of the storm's mesoscale or near-storm environment (NSE), and NOT due to the region of the U.S. that the storm is occurring. The NSE should be closely monitored during warning operations so that the proper adaptable parameter sets are always used. Keeping adaptable parameter settings at some site-selected default value because of regional expectations of a certain storm type (i.e., mini supercells always occur in the Northeast) may result in poor algorithm performance if the prevailing NSE does not correspond to the default settings. For example, if an NSE supportive of large and tall ("Oklahoma-style") supercells is occurring in New York, use the TDA adaptable parameter developed for these types of storms.

p) Based on algorithm studies and field surveys, the OSF now offers improvement to performance of the current WSR-88D Mesocyclone Algorithm (88D-MA) by allowing local radar sites the option to lower the Threshold Pattern Vector (TPV) [(1)]. This change appears to improve the probability of detecting tornadic vortices and increases the lead times for warnings in certain storm situations. [(2)]

q) Guidelines for warnings based on established thresholds for shear have limitations at far ranges. A series of mesocyclone strength nomograms (which display rotational velocity as a function of range) for three different vortex diameters are given in Figure1, Figure 2, and Figure 3. The variation of the slopes of the lines on the nomograms illustrate this range-dependency problem. The slopes become progressively steeper for the 2 nm and especially the 1 nm diameter nomograms. Meteorologists who use these nomograms should recognize that there can be considerable overlap in the strength categories for a given rotational velocity for different types of storms (smaller diameter mini supercells, for example).

3. Build 10 TDA Guidance [Top]

a. Introduction

Performance characteristics of the new Build 10 Tornado Detection Algorithm (TDA) (Mitchell et al. 1998) differ considerably from the old TVS Algorithm. The old algorithm located vertically correlated velocity maxima and minima (not necessarily gate-to-gate) anywhere within the confines of a previously-identified mesocyclone. When the old algorithm triggered in the past, tornadic events were usually already occurring. The new TDA identifies two-dimensional (2D) features, correlated in height, that contain cyclonic gate-to-gate shear. The TDA finds many three-dimensional (3D) gate-to-gate vortices that the old algorithm missed. This increased sensitivity allows the new algorithm to detect locally-intense, high-shear vortices associated with developing tornadoes. However, not all high shear vortices are associated with tornadic damage on the ground. Therefore, the TDA will trigger more frequently than the old algorithm. Build 10 TDA output, as with any algorithm, should be considered guidance. Warnings should not necessarily be issued on all TDA detections.

Forecasters should evaluate the identified velocity feature, reflectivity structure, environmental factors, and their trends before issuing a tornado warning. For a more complete comparison of the old TVS Agorithm and the Build 10 TDA Algorithm, see the WSR-88D Build 10 Training Document developed by the WSR-88D OSF Operations Training Branch.

b. Tornadic Vortex Signature (TVS)

As stated previously, forecasters should be aware that only in very rare instances can the WSR-88D actually observe the actual tornado, owing to the sampling limitations of the radar (the tornado must be very large and/or very close to the radar). In most instances, especially at longer ranges, a TVS is actually the detection of an intermediate-scale vortex or a small mesocyclone, observed as a gate-to-gate velocity couplet. Also, Trapp et al. (1998) observed that nearly 48% of all the TVS features contained in their study (based on manual detection of gate-to-gate shear) developed upward from the surface or simultaneously over a large depth (non-descending) and that about 52% descended from mid altitudes. Many descending TVS features evolved over 15 minutes. Non-descending TVS features evolved quickly (5 minutes, or about one volume scan). Most squall line tornadoes evolved quickly and were of the non-descending type. Isolated supercell tornadoes evolved in both manners.

In supercell thunderstorms, if a TVS is identified adjacent to a strong reflectivity gradient, especially near the back of a storm, near a notch, appendage, or hook on the right rear flank of a storm, then special consideration should be given for the warning decision. Strong reflectivity gradients are many times associated with strong updrafts that support tornadogenesis.

Compared to the old algorithm, the TDA detects more signatures in squall lines and along gust fronts. Forecasters should give special consideration to TDA detections that occur along leading edges of squall lines, along intersecting outflow boundaries, or within bow-echo comma heads.

Forecasters should anticipate rapid evolution, on the order of one volume scan, with line storms. TDA detections that aren't associated with these storm structures or aren't in the positions noted above are more likely not to be associated with tornadoes.

TDA may identify multiple TVSs in the same storm cell. Forecasters should not always infer a greater likelihood of tornadoes because the TDA identifies multiple TVSs that are $\leq$ 5 km of each other. Usually, there are multiple cores of tornadic shear within a strong supercell, and the TDA can isolate these cores.

The old TVS Algorithm missed most vortices, had almost zero lead time, and had no time continuity. The new algorithm, because of its greater sensitivity, provides time/space continuity and positive lead times. The new algorithm has identified TVSs nearly continuously for long-lived supercells that cyclically produced tornadoes.

Do not expect to see "drop-out gates"(missing data) in velocity products with high shear regions (e.g., mesocyclones). The Build 10 Dealiasing Algorithm has been modified so that velocity drop outs do not occur. This was implemented to give the new TDA a chance to evaluate all available velocity data, rather than skip over missing data that could contain TVSs (see the WSR-88D Build 10 Training Document).

The new algorithm can be affected by ground clutter (especially when the reflectivity threshold is set to a low number). In rare instances, the Build 10 velocity Dealiasing Algorithm will retain velocities associated with ground clutter[(3)]. Warning forecasters should be careful if false TDA detections occur in regions of ground clutter breakthrough (near the RDA or near mountainous terrain). If this situation occurs during storm events, forecasters should use extreme caution in their warning decisions, utilizing additional information such as spotter reports or radar and algorithm trends, and examine data for obvious noise.

c. Elevated TVS (ETVS)

ETVS was originally developed to fill gaps in TVS tracking and trends. Even though TVS tracking and trends were not implemented in Build 10 (yet, are available in WATADS), the computer code for ETVS detection capability was added because a) it would be eventually needed for tracking and trends (for future TDA versions in the ORPG), and b) it was felt that ETVS information, with further evaluation and refinement, could provide additional lead-time information to forecasters (see Trapp et al. 1998).Subsequent additional testing and feedback revealed that most WDSS test sites did not find ETVS information useful and had turned them off. *By default*, the display of *ETVS is turned off*.

Therefore, the OSF currently recommends that the number of ETVS's be set to zero at the UCP. Some sites may determine that by displaying the ETVSs, the increase in algorithm POD may be more important than the increase in algorithm FAR. Sites should be aware that the choice to

display ETVSs will affect private-sector users who may obtain this information through the Combined Attribute Table available from a NIDS vendor.

For a complete description of how to control the display of ETVSs and how to set other TVS adaptable parameters, see the WSR-88D Build 10 Training Document developed by the WSR-88D OSF Operations Training Branch.

d. Adaptable parameter sets

TDA has been designed to find all 3D vortices characterized with tornadic-like shear (potentially tornadic) and then filter away those not associated with tornadoes. The idea behind this concept is that stronger and deeper 3D vortices are more likely to be associated with tornadoes than weak and shallow vortices. The gate-to-gate velocity difference at the lowest radar elevation, the maximum gate-to-gate velocity difference anywhere in the 3D vortex, and the vortex depth are used in this filtering process.

OSF and NSSL personnel have defined several adaptable parameter sets to be used with the new TDA. These parameter sets define minimum threshold values of 3D Feature Low-Level (or low-altitude) Delta Velocity (LLDV), TVS Maximum Delta Velocity (MDV), and 3D Feature Depth (DPTH). These parameters have been optimized for different storm types. The definition and development of these adaptable parameter sets can be found in Lee and Mitchell, 1999.[4] Further information about adaptable parameter sets is also available in the RPG Adaptable Parameter Handbook.

Performance of the WSR-88D Build 10 TDA was optimized by calculating Probability of Detection (POD), False Alarm Ratio (FAR), and Critical Success Index (CSI) values (Wilks 1995) for many combinations of LLDV, MDV, and DPTH[5]. The combinations of adaptable parameter values that generated the best TDA performance (highest CSI and lowest FAR) were established for a an isolated supercell data set, a composite data set (default set), and a squall line data set. The isolated supercell data set (prepared after the development of the Build 10 Training Guide) only contained "traditional" strong and tall supercells. The composite data set contained "traditional" strong and tall isolated supercells, squall lines, mini supercells, and tropical-cyclone-related supercells. The squall line data set contained only squall lines. Special classes of tropical-cyclone-related cases and miniature-supercell cases were also tested to see if better performing adaptable parameter sets could be found for them. For the tropical and miniature classes, no improvement was found over using the squall line adaptable parameter set. The "squall line/other" adaptable parameter set is, therefor, intended for use with squall lines, miniature supercells, and tropical-cyclone-related supercells.

Overall performance scores are reported in Table 2. TDA performed best on the isolated supercell data set, and a decrease in skill was noted for the composite/default data set and, in particular, the squall line data set. Four adaptable parameter sets are recommended for use with TDA:

1. **Composite/Default Adaptable Parameter Set** - This set performed best on the entire data set. It is recommended for use when the storm type is mixed within the maximum range of the algorithm (or not known with much certainty) and when the user wants to stick with one adaptable parameter set and not make any changes.

2. **Isolated Supercell Adaptable Parameter Set** - This set performed best on isolated supercells (including LP, Classic, and HP varieties). It is recommended any time the weather pattern favors a preponderance of isolated supercells.

3. **Squall line/Other Adaptable Parameter Set** - This set performed best for squall line cases, tropical-cyclone-related cases, and miniature supercell cases. It is recommended for any specific storm type except isolated supercells.

4. **Minimized Adaptable Parameter Set** - This set was derived to match as closely as possible to the performance of the old Build 9 (and previous builds) TVS Algorithm. It is recommended only for situations where the need to minimize the number of overall detections and false detections supercedes the overall better performance of the other adaptable parameter sets.

Adjusting the adaptable parameter sets on the basis of Near-Storm Environment (NSE) data should provide TDA performance comparable to the levels indicated in Table 2. Some additional improvement in performance may be obtained from further local-office study *of storm types* and TVS characteristics for local areas. Future detailed studies may suggest ranges of acceptable individual parameters (within and apart from sets of parameters) from which local-office personnel could choose appropriate values to "tune" the algorithm. Such studies, utilizing the WATADS software are highly recommended. Those who perform such studies are cautioned to make sure that they have enough local cases to provide a statistically significant data set. If individual local offices have only a few cases for various storm types, they are encouraged to combine data sets with nearby offices who experience similar storm types. Until adequately-sized local data sets have been collected and analyzed, local offices are encouraged to choose between the four adaptable parameter sets presented here whose performance has been quantitatively measured.

Outside of the four adaptable parameter sets there are three site-adaptable TDA parameters that can be changed at the UCP: the Maximum Number of Elevated TVSs, the Minimum Reflectivity, and the Maximum Pattern Vector Range. The Maximum Number of Elevated TVSs can range from 0 to 25 depending on the desired TDA Algorithm performance at each site. As noted in the ETVS section, sites should be aware that choosing to display ETVSs will also impact private-sector users who may obtain this information through the combined attribute table available from a NIDS vendor.

The Minimum Reflectivity site-adaptable TDA parameter is the minimum reflectivity required for a velocity bin to be used in creating a pattern vector for TDA. The default value is set to 0 dBZ, and the adjustable values range from 0 to 20 dBZ. Using higher values will result in a decreased number of TDA detections and a slight decrease in FAR. Significant "missed detections" have occurred with 20 dBZ values, particularly with Classic-LP type storms with weak reflectivities in the hook echo.

The Maximum Pattern Vector Range is the maximum range that pattern vectors are identified for the TDA Algorithm. The default is set at 100km, and the adjustable values range from 100 to 150 km. TDA detections at far ranges should be used with caution due to radar sampling limitations.

4. Latest Statistical Results from NSSL Algorithm Development (MDA, TDA, BWER) [Top]

a. Introduction

This section presents some statistics from of the latest results from algorithm development work at NSSL. As part of this effort, 85 velocity and reflectivity parameters were statistically analyzed, for their ability to discriminate between tornadic and non-tornadic vortices in storms (descriptions for some of these radar-derived parameters are contained in Appendix A). It is understood that operational warning forecasters have considerable time limitations that prohibit examination and/or computation of many of the 85 parameters that have been measured here. This analysis is offered as important background information and as an attempt to highlight the most important parameters (or "best predictors" for diagnosing tornadic vortices), and only those best predictors which are easily determined using either algorithm output or via quick PUP or AWIPS examination.

Ideally, for the statistical analysis, one would prefer that all of these parameters be measured manually (i.e., by a radar meteorologist) to minimize errors. However, past experience at NSSL has shown that this process is very time consuming (thus, greatly limiting the amount of data that can be statistically evaluated). Instead, it has been decided to rely on the latest versions of NSSL's Mesocyclone Detection Algorithm (MDA) (Stumpf et al. 1998), Tornado Detection Algorithm (TDA) (Mitchell et al. 1998), and experimental Bounded Weak Echo Region (BWER) Algorithm to identify and measure these parameters. While this might introduce some errors into the analysis, it also allows analyses of a much larger amount of data than could be done manually. This is done with the confidence that the new NSSL algorithms are robust enough that the advantages (larger data set) of this procedure outweigh the disadvantages (additional errors).

It should be noted that only output from the NSSL TDA is available on the PUP. When any NSSL MDA parameters are presented as best predictors, each variable can either be measured manually at the PUP (e.g., using the V_r-shear function), or the corresponding 88D Mesocyclone Algorithm detection attributes can be used as a proxy. It is also shown that the only BWER Algorithm parameter that showed predictive strength was the simple existence of a BWER detection. Although there is no BWER Algorithm available on the PUP, manual reflectivity analysis (via a 4-panel display or WER product) can determine the existence of a BWER in a storm.

All of the NSSL MDA and BWER products are available via post-analysis using WATADS. They are also available to some NWS offices on NSSL's Warning Decision Support System (WDSS). WDSS users can directly utilize the NSSL MDA and BWER output rather than using PUP proxies.

What is presented here are the major results of the statistical analysis of the 43-case data set. Results take the form of a number of plots for the algorithm parameters which have been deemed the "best predictors" for tornadoes. A discussion on how to use these plots is included in the text. A technical discussion of the statistical analysis is presented in Appendix B.

b. Data

For the 43-case data set (Table 1), there were a number of MDA, TDA, and BWER detections. The following subsets of data were created to do the statistical analysis:

Subset I :	circulations detected by MDA, only.
Subset II :	circulations detected by TDA, only.
Subset III :	circulations detected by MDA and TDA, jointly.
Subset IV :	circulations detected by MDA and BWER, jointly.
Subset V :	circulations detected by TDA and BWER, jointly.
Subset VI :	circulations detected by MDA, TDA, and BWER, jointly.

The entire data set constitutes 43 days of storm data (Table 1). The MDA data consist of all MDA detections that are of Strength Rank ≥ 1 [see Stumpf et al. (1998) or Appendix A for a definition of Strength Rank]. The TDA data consist of all TDA detections whose low-altitude and mid-altitude gate-to-gate velocity differences are at least 11 m s^{-1}. All MDA and TDA detections are either associated with tornadoes (if a tornado occurred during the previous 5 or 6 minute volume scan, is occurring in the present volume scan, or will occur within 20 minutes from the present volume scan), or not (called "non-tornadoes")[(5)]. Both algorithms used a 0 dBZ threshold for the Minimum Reflectivity adaptable parameter.

The total sample size, N, the number of non-tornadoes, N_0, the number of tornadoes, N_1, and the *a-priori* probability (i.e. climatological, and *prior* to additional statistical analysis) of tornado, $p1 = N_1/N$, in each of these subsets is given in Table 3. Also included is the number of attributes (independent variables) in each subset.

Even without any analysis, the *a priori* probability (i.e., *prior* to additional statistical analysis) of tornado for the six subsets (Table 3) offers a useful guidance. An MDA detection of Strength Rank greater than or equal to five (the "Mesocyclone" classification), and a TDA detecgion meeting the Default-TVS parameters in Table 2, separately, have a relatively low probability of being tornadic (i.e., 10.4% and 6.3% respectively); a joint detection of a Mesocyclone and a Default-TVS has a 31% probability of being tornadic. This probability is raised to 38% if the joint MDA/TDA detection is also accompanied by a BWER. In other words, a circulation detected by both MDA and TDA, or by all three algorithms (MDA, TDA, BWER) should be given serious consideration as being tornadic. Therefore:

- **Any radar signature which has both a Mesocyclone and a Default-TVS detection should be given serious consideration as being tornadic.**

Of the subsets that included the BWER Algorithm output, it was found that none of the "best predictors" were BWER attributes. Therefore, for this document, results from subsets IV, V, and VI are not included. However, it is still important to note, given the 38% climatological probability that any signature with an MDA, TDA, and BWER detection is tornadic, that:

- **Even more consideration should be given to signatures with both an MDA detection, a TDA detection, and an analyzed BWER (or BWER detection is made using the WDSS).**

c. The best predictors

Using the statistical analyses presented in Appendix B, Table 4 lists the variables which have been identified as "best predictors" for diagnosing tornadoes from MDA and TDA Algorithm output. These are the variables, from the summary in Appendix B, which can be directly computed from the PUP or WDSS, or are available from the Build 10 TDA. The WDSS variables should only be used during warning operations if your office is equipped with a WDSS (although, these variables can be examined in post-analysis using WATADS). Table 4 is an interactive table with links to probability plot figures and links to decision threshold figures for each of the best predictors. Appendix A contains a description of each of the best predictors, and ways to compute these from the PUP. Table 4 also provides links to each of the variable descriptions in Appendix A.

Probabilities generated for each parameter are based on the number of tornadic circulations (defined as a circulation where a tornado has occurred in the last 5 or 6 minute volume scan, is occurring, or will be occurring within the next 20 minute period) divided by the total number of circulations detected (Eq. 1 in Appendix B).

The range of values of the decision threshold over which performance is maximized is also given in Table 4. The decision threshold is the lowest value at which decision is made if the measured attribute falls at or above the threshold. For example, if the decision threshold for a parameter is 30, then one should give special consideration for issuing a warning for values **at or above** 30. The two exceptions are indicated by the * (base parameters), in which the special consideration should be given to values at or *below* the threshold. The variables marked with ** are only available via the WDSS or WATADS. Note that the decision threshold is given as a range of values. This is range at which the Heidke Skill Statistic (HSS) reaches a high "plateau" of values.[5] We suggest that the threshold be chosen which maximizes the Probability of Detection (POD) or minimizes the False Alarm Ratio (FAR). The reader should also note that the thresholds in Table 4 were determined by maximizing HSS for each variable independently, while the TDA adaptable parameter set study considered maximizing CSI for combinations of variables. Hence, some parameters, such as TDA depth, differ substantially from Table 4 to Table 2.

These decision threshold values should be used as *guidance* during the warning process. They should not be used as "magic values" to make warning decisions. However, when the values are at least those values within the threshold ranges, special considerations should be given for warning. As always, the information should be integrated with the other data inherent in the integrated warning system.

Please use the links to the appropriate variable descriptions in Table 4 to determine how to use each variable during tornado warning operations.

5. Summary [Top]

Issuing tornado warnings remains a difficult but critical task for operational forecasters. Besieged by an increasing amount of information, a National Weather Service meteorologist in a "warning situation" usually depends on radar data to help make the final decision on whether or not to warn.

This document has summarized some of the cutting edge tornado hypotheses from the basic and applied research community with the warning forecaster in mind. These ideas are constantly in flux, as new data are gathered, and as old data are thought of in different ways. Look to future editions of this Tornado Warning Guidance for the latest in these research results.

This document also presents additional information for the new Build 10 Tornado Detection Algorithm (TDA) to compliment the Build 10 Training Guide. Use them in concert.

In an attempt to determine which of 85 radar-derived independent variables could best discriminate between tornadic and non-tornadic vortices, a total of 43 unique storm cases were analyzed using the NSSL MDA, TDA, and BWER. For the 2nd Edition of the Tornado Warning Guidance, the statistical analysis results differ quite a bit from what was published in Edition 1. Gone is the notion of using Linear Discriminant Analysis (LDA) to determine best predictors. Since the 1st Edition, two more years of statistical research have been conducted, and new better ways to analyze the data are now known. This document contains some of those cutting edge ideas (some of which have not yet been formally published). Through a variety of methods, a number of “best predictors” have been determined from both mesocyclone and TVS detection, which should be considered when issuing tornado warnings. A brief summary of how each of these radar-derived parameters was calculated and the physical significance of some is presented in bullet text form in Appendix A. Threshold values for many of the “best predictors” are shown in Table 4, and the graphs of performance and probabilities used to determine the thresholds are provided in graphs PT1-PT15.

In the future, the statistics presented in Section 4 may be stratified by range and storm-type. A subset of the 43-cases is currently being developed which includes Near-Storm Environment (NSE) data from the Rapid Update Cycle (RUC-1) mesoscale model. NSE data is paramount to the integrated warning system, and it is hoped that the NSE data, coupled with MDA, TDA, and BWER output, will provide more clues for tornado warning guidance.

Our best guidance on using WSR-88D data in the tornado warning decision-making process continues to be to closely examine the base data and use all three Doppler moments together (reflectivity, velocity, and spectrum width). The supporting algorithms (Mesocyclone and TDA) supply initial information about where to look, important guidance about quantitative signature parameter values, and help prevent failure to interrogate all important storms. However, the algorithms are not highly skilled enough for stand-alone use. For TDA, it is recommended to use adaptable parameter sets of known skill score. Special consideration should be given to situations where a TVS is detected in conjunction with a storm that already has a mesocyclone signature detection. If the storm has a recognizable three-dimensional, supercell structure (BWER, developing

hook echo, etc), even greater consideration should be given for a tornado warning with that storm. The statistics in this document have shown that detection of signatures by totally independent algorithms and by data in multiple Doppler moments is a powerful tool in highlighting which storms are more likely to produce tornadoes.

Further improvement in the Mesocyclone and TDA Algorithms is possible by tuning them to the type and character of storms which are a function of the near-storm environment. New and improved adaptable parameter sets and ranges of values for individual adaptable parameters are likely to be found for different storm types. Those involved in regional or local studies (most likely with WATADS) are encouraged to develop data sets large enough to ensure that the analysis produces statistically significant results.

Users should note that the statistics were based on a fairly small number of storm days (43 days), and, they represent an overall composite of all the storms analyzed. The actual probability that a given storm being viewed by a WSR-88D will produce a tornado may be much higher or lower. None of the data should in any way be used as "magic values" for issuing warnings. One should **always** use **all** available data sources (including reflectivity data trends, spotter reports, storm history, and the mesoscale environment) before making a final decision on whether or not to issue a tornado warning.

If you have any feedback for this document, please contact the editors or one of the contributors in the points-of-contact list. While every attempt has been made to create a complete document, the users in the field, with first hand experience issuing tornado warnings, have a wealth of experience that can significantly enhance future versions of the Tornado Warning Guidance Document. Users' contributions to this knowledge base is invaluable, and sites are strongly encouraged to share datasets and findings with the OSF and NSSL.

6. Bibliography [Top]

Brooks, H. E., C. A. Doswell III, and R. B. Wilhelmson, 1994: The role of midtropospheric winds in the evolution and maintenance of low-level mesocyclones. *Mon. Wea. Rev.*, **122,** 126-136.

Brooks, H. E., C. A. Doswell III, M. T. Carr, and J. E. Ruthford, 1996: Preliminary analysis of soundings from VORTEX-95. *Preprints, 18th Conf. on Severe Local Storms,* San Francisco, CA, Amer. Meteor. Soc., 133-136.

Burgess, D. W., R. L. Lee, S. S. Parker, S. J. Keighton, and D. L. Floyd, 1995: A Study of mini supercells observed by WSR-88D radars. Preprints, *27th Conf. on Radar Meteorology*, Vail, CO, Amer. Meteor. Soc., 4-6.

Burgess, D. W., and M. A. Magsig, 1998: Recent observations of tornado development at near range to WSR-88D radars. *Preprints,19th Conf. on Severe Local Storms,* Minneapolis, MN, Amer. Meteor. Sci., 756-759.

Gandin, L. S., and A. Murphy, 1992: Equitable skill scores for categorical forecasts. *Mon. Wea. Rev.*, **120**, 361-370.

Grant, B. N., and R. Prentice, 1996: Mesocyclone characteristics of mini supercell thunderstorms. Preprints, *15th Conf. On Wea. Anal. and Forecasting*, Norfolk, VA, Amer. Meteor. Soc., 362-365.

Lee, R. R., 1995: Improvement of the WSR-88D Mesocyclone Algorithm. Documentation available from the WSR-88D Operational Support Facility/Application Branch, Norman, OK, 73069, 44 pp.

Lee, R. R., and E. D. Mitchell, 1999: Performance of The WSR-88D Build 10 Tornado Detection Algorithm: Development of Optimal Adaptable Parameter Sets. *Preprints, 15th Intl. Conf. on Interactive Information and Processing Systems (IIPS) for Meteorology, Oceanography, and Hydrology,* Amer. Meteor. Soc., Dallas, TX, in press.

Lee, R. R., A. White, 1998: Improvement of the WSR-88D Mesocyclone Algorithm. *Wea. Forecasting*, **13**, 341-351.

Lee, R., R., G. J. Stumpf, and P. L. Spencer, 1998: Should geographic region or near-storm environment dictate WSR-88D algorithm adaptable parameter settings? *Preprints, 19th Conf. on Severe Local Storms,* Minneapolis, MN, Amer. Meteor. Sci., 784-787.

Markowski. P. M., E. N. Rasmussen, J. M. Straka, 1998: The occurrence of tornadoes in supercells interacting with boundaries during VORTEX-95. *Wea. Forecasting*, **13**, 852-859.

Markowski, P. M., J. M. Straka, E. N. Rasmussen, D. O. Blanchard, 1998: Variability of Storm-Relative Helicity during VORTEX. *Mon. Wea. Rev.*, **126**, 2959-2971.

Marzban, C. and G. J. Stumpf, 1996: A neural network for tornado prediction based on Doppler radar-derived attributes. *J. Applied Meteor.*, **35**, 617-626.

Marzban, C., 1998a: Scalar measures of performance in rare-event situations. *Wea. Forecasting*, **13**, 483-493.

Marzban, C., 1998b: Bayesian probability and scalar performance measures in Gaussian Models. Journal of Applied Meteorology, **37**, 72.

Marzban, C., and V. Lakshmanan, 1998: On the Uniqueness of Gandin and Murphy's Equitable Performance Measures. *Mon. Wea. Rev.*, in press.

Marzban, C., G. J. Stumpf, and E. D. Mitchell, 1998: What are the best predictors of tornadoes?. *Preprints,19th Conf. on Severe Local Storms*, Minneapolis, MN, Amer. Meteor. Sci., 729-732.

Marzban, C., E. D. Mitchell, and G. J. Stumpf, 1999: On the Notion of "Best Predictors:" An Application to Tornado Prediction. Submitted to *Wea. Forecasting*.

Mitchell, E. D., S. V. Vasiloff, G. J. Stumpf, A. Witt, M D. Eilts, J. T. Johnson, K. W. Thomas, 1998: The National Severe Storms Laboratory Tornado Detection Algorithm. *Wea. Forecasting*, **13,** 352-366.

Mitchell, E., D., and K. L Elmore, 1998: A Severe Weather/Tornado Climatology Using the WSR-88D. *Preprints,19th Conf. on Severe Local Storms*, Minneapolis, MN, Amer. Meteor. Sci., 273-275.

Operational Support Facility, 1998: WSR-88D Build 10 Training. Available on the Web at: http://www.osf.noaa.gov/otb/build10/nexrad.htm

Rasmussen, E. N., J. M. Straka, R. Davies-Jones, C. A. Doswell III, F. H. Carr, M. D. Eilts, and D. R. MacGorman, 1994: Verification of the origins of rotation in tornadoes experiment: VORTEX. *Bull. Amer. Meteor. Soc.*, **75,** 995-1006.

Stumpf, G. J., 1998: Operational Paradigms of Automated Storm-scale Vortex Detection: Lessons Learned and Future Thoughts. Available on the Web at: http://www.nssl.noaa.gov/~farmer/internal/presentations/vddaabr.html

Stumpf, G. J., A. Witt, E. D. Mitchell, P. L. Spencer, J. T. Johnson, M. D. Eilts, K. W. Thomas, D. W. Burgess, 1998: The National Severe Storms Laboratory Mesocyclone Detection Algorithm for the WSR-88D. *Wea. Forecasting*, **13**, 304-326.

Stumpf, G. J., E. D. Mitchell, K. L. Elmore, V. T. Wood, P. C. Burke, and K. T. Angle, 1998: The new NSSL Vortex Detection and Diagnosis Algorithm - plans, status, issues. *Preprints, 19th Conf. on Severe Local Storms,* Minneapolis, MN, 725-728.

Stumpf, G. J., P. C. Burke, and E. D. Mitchell, 1999: SWAT's WSR-88D Mesocyclone and Tornado Signature Case Study Page. Available on the Web at: http://www.nssl.noaa.gov/swat/Cases/cases_pix.html

Trapp, R. J., and E. D. Mitchell, 1995: Characteristics of tornadic vortex signatures detected by WSR-88D radars. *Preprints, 27th Conf. on Radar Meteorology,* Vail, CO, Amer. Meteor. Sci., 211-212.

Trapp, R. J., E. D. Mitchell, G. A. Tipton, D. A. Effertz, A. I. Watson, D. L. Andra, and M. A. Magsig, 1998: Descending and non-descending tornadic vortex signatures detected by WSR-88Ds. *Preprints, 19th Conf. on Severe Local Storms,* Minneapolis, MN,128-131.

Wilks, D. S., 1995: *Statistical Methods in the Atmospheric Sciences*. Academic Press, 467 pp.

Wood, V. T., and R. A. Brown, 1997: Effects of radar sampling on single-Doppler velocity signatures of mesocyclones and tornadoes. *Wea. Forecasting,* **12**, 928-938.

Witt, A., M. D. Eilts, G. J. Stumpf, E. D. Mitchell, J. T. Johnson, and K. W. Thomas, 1998: Evaluating the performance of WSR-88D severe storm detection algorithms. *Wea. Forecasting*, **13**, 513-518.

Footnotes [Top]

1. The adaptable parameter TPV controls the minimum number of Pattern Vectors needed for identification of a 2-D feature in the 88D-MA. A Pattern Vector is defined as a continuous run of azimuthally adjacent radial velocities with increasing values (from max outbound to max inbound). Lowering TPV [to a value between 6 and 10 (inclusive)] increases detection of smaller mesocyclones. Return to text.

2. For more information on how these adaptable parameter changes affect algorithm skill, contact Bob Lee at the OSF Application Branch. Return to text.

3. Recent testing by the OSF Applications Branch has identified a rare situation under which the TDA may produce a large number of false alarms. The scenario is as follows: Poor receiver calibration (i.e., A/D saturates before the automatic gain control steps in) can reduce the effectiveness of clutter suppression. This clutter, when mixed with return from strong thunderstorms (dBZ > 40 to 45), will cause the velocity Dealiasing Algorithm to speckle the velocity field with bins of near zero velocity. The TDA may identify pairs of velocity bins that satisfy the criteria for TVSs. Under these circumstances the TDA may produce a large number of false alarms (six or more TVSs have been observed within a volume scan while a storm was passing over a WSR-88D site). More information about this phenomena is available from Dave Zittel at the OSF Applications Branch. Return to text.

4. The parameter values published in Lee and Mitchell 1999 are slightly different from the values presented in Table 2 and in the WSR-88D Build 10 Training manual. Forecasters should use the values in Table 2. Return to text.

5. Certain (mostly earlier) portions of this document are based on CSI, while other (mostly later) portions are based on a different measure of performance, called Heidke Skill Statistic (HSS). This change in the measure of performance was done because HSS has lately emerged as a "better" measure of performance. The most important difference is that HSS incorporates the correct forecasts of nonevents, while CSI does not. The reasons for using CSI are mostly historical. In fact, only recently has it been shown that CSI has certain inadequacies. To elaborate further, it has been shown in (Gandin and Murphy 1992, Marzban 1998a, Marzban and Lakshmanan, 1998) that CSI is pathological in many respects, one of which is its "inequitability." Briefly, the use of an inequitable measure can cause a forecaster to "hedge" the forecasts. For example, in the context of the finding thresholds that maximize a measure of performance, the inequitability of the measure can cause the optimal value of the threshold to be the lowest (or highest) value of the variable itself. As such, severe over- or under-forecasting can occur (see Appendix B). For such reasons, it was deemed necessary to replace CSI as a measure of performance with HSS.
Return to text in Section 3. Return to text in Section 4. Return to Table 2.

6. STORM DATA was used as either the partial or complete verification source for all cases in this study. In some cases, data sets from VORTEX or other well-done damage surveys were used to

supplement the STORM DATA report. This study, like most others, is limited by accuracy of the verification data. Return to text.

APPENDIX A [Top]

Summary of Algorithm Parameter "best predictors"

Please refer to Appendix C to match the parameter name and description to the parameter numbers presented in Section 4. The first 15 parameters are those listed as "best predictors" in Table 4. These parameters are listed in no particular order. Stumpf et al (1998) and Mitchell et. al (1998) describe these parameters (for the MDA and TDA respectively) in much greater detail.

Subset I (MDA only):

MDA Depth

The total depth (m) of the 3D feature in NSSL MDA is calculated by adding the half-power beamwidth to the top and the base of the meso feature. A depth of least 3 km has often been cited as a minimum threshold depth for mesocyclones that produce tornadoes. However, on the average, mini-supercells can have mesocyclone depths that are somewhat less (2.4-2.6 km). The 88D-Mesocyclone Algorithm value on the PUP can serve as a proxy for this parameter. This parameter is available on WATADS/WDSS in the MDA Table. As the value of this parameter increases, so does the probability of tornado.

MDA Strength Rank

It is a ranking (1-25) in NSSL MDA based on the strongest continuous "core" of mesocyclone features (3 km deep, base < 5 km AGL) of a given strength rank. The original strength rank of the 2D MDA feature is computed using max rotational velocity difference and shear in an identified pattern vector. The "Strength Rank" is akin to assigning increasing numerical values to the regions in the mesocyclone nomogram (but uses slightly different criteria and more regions). A complete explanation of this parameter is available in Stumpf et al. (1998). As the value of this parameter increases, so does the probability of tornado. *This parameter is only available on WATADS/WDSS in the MDA Table.*

MDA Maximum Rot. Velocity

The calculation is similar to low-altitude rotational velocity except for the maximum value of all 2D features used to create the 3D MDA detection. Max. values of rotational velocity for a given storm displayed on the PUP can be computed by looking at the Vr shear function at multiple slices in a storm. Otherwise, this parameter is available on WATADS/WDSS in the MDA Table. Remember that the vortex sampling limitations with range mean that lower values of this parameter at greater ranges can be significant. As the value of this parameter increases, so does the probability of tornado.

MDA Age of mesocyclone

Longer-lived mesocyclones have been shown to produce more tornadoes and travel farther than shorter-lived mesocyclones. For warning purposes, the history of a given storm is very important in terms of what the storm has done (i.e., has this meso already produced a tornado?). Although this parameter is not available on the PUP, one could manually keep track of the age of a particular mesocyclone. On WATADS/WDSS, use the number of white dots representing the previous positions of the mesocyclone, and multiply by the volume scan update rate (5 or 6 minutes) to determine the age. As the value of this parameter increases, so does the probability of tornado.

MDA Mesocyclone Strength Index (MSI)

An integrated rotational strength index from NSSL MDA, it is computed by vertically integrating the strength ranks (multiplied by 1000) of all the 2D features used to create the 3-dimensional (3D) feature. It is normalized by dividing by the depth of integration. A complete explanation of this parameter is available in Stumpf et al. (1998). As the value of this parameter increases, so does the probability of tornado. *This parameter is only available on WATADS/WDSS in the MDA Table.*

Subset II (TDA only):

TDA Base

Defined as the lowest elevation height (AGL) of the 2D TDA feature. This parameter is available in the TDA table on the PUP or WATADS/WDSS. Note that the probability of a tornado being produced by a storm increases steadily as the TVS base (lowest altitude of the TVS circulation) decreases. Although the HSS is maximized at a base higher than "zero", interpret this number as the highest value at which to consider taking action, and that all value at or below this warrant special consideration.

TDA Depth [DPTH]

The total depth (m) of the 3D feature in NSSL TDA is calculated by adding the half-power beamwidth to the top and the base of the meso feature. This parameter is available in the TDA table on the PUP or WATADS/WDSS. As the value of this parameter increases, so does the probability of tornado.

TDA low-altitude gate-to-gate delta-V [LLDV]

Defined as the gate-to-gate delta-v (m/s) at the lowest elevation slice of the 3D TDA feature, such as 0.5 or 1.5 degree slice. This parameter is available in the TDA table on the PUP or WATADS/WDSS. Remember that the vortex sampling limitations with range mean that lower

values of this parameter at greater ranges can be significant. As the value of this parameter increases, so does the probability of tornado.

TDA maximum gate-to-gate delta-V [MDV]

Defined as the maximum gate-to-gate delta-v (m/s) of all the 2D TDA features comprising the 3D feature. This parameter is available in the TDA table on the PUP or WATADS/WDSS. Remember that the vortex sampling limitations with range mean that lower values of this parameter at greater ranges can be significant. As the value of this parameter increases, so does the probability of tornado.

Subset III (MDA+TDA only):

*Special note: Use these parameters **only** when an MDA detection and TDA detection are both found for the same radar vortex signature. Note that the decision threshold values the three TDA parameters is different when using them for vortex signatures where only a TDA detection is present.*

MDA Low-altitude Diameter

Defined as the diameter (m) from the lowest elevation 2D MDA feature. The diameter corresponds to the distance between the peak radial velocities used to calculate rotational velocity. This could be computed manually using the Vr Shear function on the PUP. Otherwise, this parameter is available on WATADS/WDSS in the MDA Table. As the value of this parameter increases, so does the probability of tornado.

MDA Low-altitude Rot. Velocity

This particular parameter was calculated from the lowest elevation slice that the 3D MDA detection was found (note: it is NOT always at 0.5 degrees). A similar quantity can be computed at the WSR-88D PUP by using the Vr shear function on the maximum inbound/outbound velocity couplet sampled at a particular elevation slice. Computed by Vr shear function on the SRM or SRR product at the lowest elevation angle, such as 0.5 or 1.5 degree slice. Otherwise, this parameter is available on WATADS/WDSS in the MDA Table. Remember that the vortex sampling limitations with range mean that lower values of this parameter at greater ranges can be significant. As the value of this parameter increases, so does the probability of tornado.

MDA Low-altitude g-g del v

Defined as the gate-to-gate delta-v (m/s) at the lowest elevation slice of the 3D MDA feature, such as 0.5 or 1.5 degree slice. This can be manually determined using the PUP. Otherwise, this parameter is available on WATADS/WDSS in the MDA Table. Remember that the vortex sampling

limitations with range mean that lower values of this parameter at greater ranges can be significant. As the value of this parameter increases, so does the probability of tornado.

MDA Core Base

Defined as the height (AGL) of the lowest-elevation 2D "core" feature from NSSL MDA. (Note: a "core" as defined in NSSL MDA is based on strength rank. The core must be at least 3 km deep with the base below 5 km and top at or below 8 km). Use the base of the 88D-Mesocyclone Algorithm detection as a proxy to this number. Otherwise, this parameter is available on WATADS/WDSS in the MDA Table as “BASE”. Note that the probability of a tornado being produced by a storm increases steadily as the mesocyclone base (lowest altitude of the mesocyclone circulation) decreases. Although the HSS is maximized at a base higher than “zero”, interpret this number as the highest value at which to consider taking action, and that all value at or below this warrant special consideration.

TDA low-altitude gate-to-gate delta-V [LLDV]

Defined as the gate-to-gate delta-v (m/s) at the lowest elevation slice of the 3D TDA feature, such as 0.5 or 1.5 degree slice. This parameter is available in the TDA table on the PUP or WATADS/WDSS. Remember that the vortex sampling limitations with range mean that lower values of this parameter at greater ranges can be significant. As the value of this parameter increases, so does the probability of tornado. *Note that the decision threshold values for this TDA parameter, when there is an MDA and TDA detection present, is different when using them for vortex signatures where only a TDA detection is present.*

TDA maximum gate-to-gate delta-V [MDV]

Defined as the maximum gate-to-gate delta-v (m/s) of all the 2D TDA features comprising the 3D feature. This parameter is available in the TDA table on the PUP or WATADS/WDSS. Remember that the vortex sampling limitations with range mean that lower values of this parameter at greater ranges can be significant. As the value of this parameter increases, so does the probability of tornado. *Note that the decision threshold values for this TDA parameter, when there is an MDA and TDA detection present, is different when using them for vortex signatures where only a TDA detection is present.*

These three remaining parameters were not found to be "best predictors" for the 1999 statistical analysis, but they showed high predictive strength in the 1997 analysis, and they have shown to be of particular importance to the warning guidance process. The reason the first two values here were not "best predictors" probably results from the fact that a small percentage of mesocyclones are close enough to the radar for these low-altitude phenomena to be measured.

MDA Low-altitude Convergence

Calculated in this analysis of NSSL MDA data as the average radial convergence (avg. delta-v) measured within the diameter (plus 2 km) of each 2-dimensional (2D) circulation feature analyzed between 0 and 2 km (AGL) in the 3D detection. A similar value could be manually computed at the PUP via the Vr shear function. Low-altitude convergence is often noted below the base of a mesocyclone in its organizing stage. This parameter is not available on WATADS/WDSS.

MDA Mid-altitude Convergence

It is calculated the same as low-altitude convergence, except for 2D MDA features that are at 2 to 4 km (AGL). This parameter is not available on WATADS/WDSS.

TDA Tornado Strength Index (TSI)

This is computed by vertically integrating the gate-to-gate delta-V of all 2D TDA features used to create the 3D feature. It is normalized by dividing by the depth of integration. This parameter is similar to the Average Delta-V (AVDV) parameter that is available in the TDA table on the PUP. Remember that the vortex sampling limitations with range mean that lower values of this parameter at greater ranges can be significant. It is available on WATADS/WDSS in an ascii text file. As the value of this parameter increases, so does the probability of tornado.

APPENDIX B [Top]

Technical discussion of statistical analysis of NSSL algorithm parameters

a. Analysis

The following analysis was performed to re-evaluate the question "What can the radar-algorithm data offer in the way of guidance for a tornado forecaster?" More specifically, an attempt was made to identify the particular variables that appeared to be the best predictors of tornadoes. Many of the subtleties of that question have been extensively addressed in Marzban et al. (1999), and so only a mention of them will be made herein.

Six data subsets will be examined:

Subset I :	circulations detected by MDA, only.
Subset II :	circulations detected by TDA, only.
Subset III :	circulations detected by MDA and TDA, jointly.
Subset IV :	circulations detected by MDA and BWER, jointly.
Subset V :	circulations detected by TDA and BWER, jointly.
Subset VI :	circulations detected by MDA, TDA, and BWER, jointly.

The total sample size, N, the number of non-tornadoes, N_0, the number of tornadoes, N_1, and the *a-priori* probability (i.e. climatological, and *prior* to additional statistical analysis) of tornado, $p1 = N_1/N$, in each of these subsets is given in Table 3. Also included is the number of attributes (independent variables) in each subset.

The entire data set constitutes 43 days of storm data (Table 1). The MDA data consist of all MDA detections that are of Strength Rank ≥ 1 [see Stumpf et al. (1998) for a definition of Strength Rank]. The TDA data consist of all TDA detections whose low-altitude and mid-altitude gate-to-gate velocity differences are at least 11 m s^{-1}. All MDA and TDA detections are either associated with tornadoes (if a tornado has occurred in the last 5 or 6 minute volume scan, is occurring, or will occur in 20 minutes from the volume scan of the detection), or not (called "non-tornadoes")[(6)]. Both algorithms used a 0 dBZ threshold for the Minimum Reflectivity adaptable parameter.

As discussed in (Marzban et al. 1999), most users of MDA or TDA rely mostly on a mental model to guide them in interpreting the output of these algorithms. As a result, they do not rely on an analytic model (e.g., regression) to which one can apply a host of statistical techniques designed to address the question of best predictors. Even when a model does exist (like the neural network), that question is a thorny one, at best; the absence of a model renders the question even thornier. For such reasons, the question of best predictors is often best answered in a bi-variate fashion, i.e. one independent variable (and one dependent variable) at a time.

In this document, several such approaches will be employed to address the question of determining the best predictors of tornadoes.

b. Methods

i. Posterior Probability Method

A first approach is to examine the posterior probability of a tornado, given the value of an independent variable, $P_1(x)$. This probability can be calculated from the conditional frequency distribution, $N_i(x)$, at a given value of x, where i = 0,1 refers to non-tornadoes and tornadoes, respectively. Specifically, Bayes' theorem (Marzban 1998b) implies

$$P_1(x) = \frac{N_1(x)}{N_1(x) + N_0(x)}, \qquad (1)$$

where

$P_1(x)$ = probability that a given value of x corresponds to a tornadic circulation,
$N_0(x)$ = number of nontornadic circulations at a given value of x,
$N_1(x)$ = number of tornadic circulations at a given value of x, and
$N = N_1 + N_0$ = total number of circulations.

A "good" predictor is one whose $P_1(x)$ changes significantly as a function of x. Three examples - two, of a "good" predictor, and one of a "bad" predictor - are given in Figure 4. The curve without the 0's and 1's is $P_1(x)$ as a function of x, and the other two curves are the (normalized) probability density functions for tornadoes (1), and non-tornadoes (0). In this way, it is possible to assess the predictive strength of each variable according to the change in $P_1(x)$ over the range of x. Note the nonlinear behavior of $P_1(x)$ in the middle plot. The plots for every predictor are not all shown, as there are just too many. Instead, in the next subsection, information is provided about which variables are considered the "best predictors" of tornadoes.

ii. Correlation Method

Another method for assessing the predictive strength of the variables is to examine their correlations with the dependent variable (i.e. tornado ground truth), specifically, Pearson's correlation coefficient, r. When both the independent and the dependent variable are continuous, r is a measure of linear correlation between the two. Although in the current case the dependent variable is binary (tornado/no-tornado), r does still offer a measure of correlation, although a better description may be association. One limitation of this method is that "nonlinear" variables, such as variable trends (see the middle plot in Figure 4), will be assigned a low predictive strength, because r is a measure of linear correlation.

iii. Measures-based Method

An alternative approach is offered by considering the way in which a forecaster uses the variables. The forecaster may be interested in issuing forecasts that optimize some categorical measure of performance. To compute a categorical measure, the variable must be dichotomized, and this can be done by introducing a decision threshold. For every value of the threshold one can compute the corresponding value of the measure. Varying the threshold over the full range of the variable will yield a corresponding change in the measure. The maximum value of the measure offers a gauge of the predictive strength of the corresponding variable. Consequently, the question of the best predictors becomes one of ordering the variables according to the maximum value of some measure of performance that can be obtained by dichotomizing each variable. Three measures will be examined here: the Critical Success Index (CSI), the Heidke Skill Statistic (HSS), and Entropy (ENT). Because each measure captures a different aspect of performance quality, the choice of the best predictors may depend on the choice of the measure. (The definitions of these measures are available in Appendix D, or upon request from Caren Marzban.) As in the previous method, this method too should be restricted to linear variables; it assigns a low predictive strength to "nonlinear" variables, because such variables would ideally require two thresholds to mark the boundaries between "warning" and "no warning."

iv. Correlations among predictors

Additionally, it is important to identify the variables - good or bad - that are correlated with one another. In this way one can further reduce the number of variables that must be examined. Pearson's correlation coefficient, *r*, can again be utilized to this end. However, the rare-event nature of the data sets under study can cause *r* to be excessively large. For this reason the correlation coefficients must be computed for the two classes (non-tornadoes and tornadoes), separately. The variables that are highly correlated for both classes may be considered statistically equivalent.

v. Linear Discriminant Analysis (LDA)

Finally, even though it has been argued (above) that the users rely mostly on a mental model for guidance in issuing warnings, one may still explore the question of predictive strength within the confines of a statistical model. In the 1st Edition of the Tornado Warning Guidance, Linear Discriminant Analysis (LDA) was employed for this purpose. However, an LDA analysis of the current data sets has revealed that the collinearity among the variables renders all measures of predictive strength (in LDA) entirely ambiguous. As a result, although the results of the analysis are available upon request, no further mention of LDA will be made herein.

c. Results

i. Preliminaries

Even without any analysis, the *a priori* probability (i.e., *prior* to additional statistical analysis) of tornado for the six subsets (Table 3) offers a useful guidance. An MDA detection of Strength Rank greater than or equal to five (the "Mesocyclone" classification), and a TDA detecgion meeting the Default-TVS parameters in Table 2, separately, have a relatively low probability of being tornadic (i.e., 10.4% and 6.3% respectively); a joint detection of a Mesocyclone and a Default-TVS has a 31% probability of being tornadic. This probability is raised to 38% if the joint MDA/TDA detection is also accompanied by a BWER. In other words, a circulation detected by both MDA and TDA, or by all three algorithms (MDA, TDA, BWER) should be given serious consideration as being tornadic. With additional analysis of the various attributes associated with each algorithm's detection, the *posterior* probability (*posterior* - meaning "after" more analysis is done), that the radar signature is associated with a tornado, can be increased.

The following analyses were performed on all six subsets of data. Of the subsets that included the BWER Algorithm output, it was found that none of the "best predictors" were BWER attributes. The sample size for the BWER sets is much smaller than the non-BWER sets, and is currently too small for an accurate determination of "best predictors". It is important, however, to realize that just the presence of a BWER increases the likelihood that the radar signature is tornadic (as stated above). Future statistical analysis may merge the BWER sets with the non-BWER sets, and use only one BWER attribute, the Overall Confidence factor (0-100%). For the non-BWER data, the Overall Confidence factor will just be set to 0%. Therefore, for this document, results from subsets IV, V, and VI are not included (please contact Caren Marzban of the contributors if more details are desired).

The attributes (variables) in each of the first three subsets are defined and numerically labeled in Appendix C. Henceforth, each of these variables will be referred to by the corresponding number.

ii. Posterior Probability Method Results

The posterior probability and the histograms are too numerous to include in this report; there are as many as the number of attributes for each subset (the right most column in Table 3), i.e. 143 (for subsets I, II, and III), three of which are shown in Figure 4. However, a tedious examination of all of these figures has led to a summary table (Table 5). The table classifies (in no particular order) the various attributes of each subset into three classes, "poor", "fair", and "good" according to a subjective interpretation of how drastically the posterior probability changes with the variable. In contrast to the other two methods, this method can reliably assign a predictive strength to "nonlinear" variables. A consequence of this classification scheme is the disadvantage of not having the capability to quantify the predictive strengths in terms of a scalar (i.e. one-dimensional) quantity. As a result, the classification of the various attributes in Table 5 is somewhat subjective.

iii. Correlation Method Results

The correlation coefficients, *r*, between ground truth and each of the variables in all the six subsets are displayed in Figure 5. A positive (negative) value of *r* means that higher (lower) values of the

corresponding variable are associated with tornadoes. The red error bars on the upper right of each plot are the one-standard deviation error bars. As seen from the plots, there are no "outstanding" predictors. In other words, many of the variables have approximately the same value of *r*. In order to isolate a set of best predictors, one can sort the *r*'s in order of magnitude, and select the variables whose *r*'s stand above the rest. An example of this is shown in Figure 6 where the *r*'s of the 53 variables in MDA (subset I) are ordered according to their magnitude. The "best" predictors of tornadoes are (see Appendix C, for numbering): 20, 53, 27, 4, 8, 21, 25, 14, all with approximately equal predictive strengths. It is worth mentioning that most of these variables are "independent" in that the correlation coefficient between any pair of them is not exceedingly high. In fact, only one pair - 53 and 25 - are highly correlated (r_0=0.948, r_1=0.950). The scatter plot between the two is shown in Figure 7. The best predictors according to this method are tabulated in Table 6, in order of their (statistically non-significant) predictive strength.

iv. Measures-based Method Results

As for the measure-based method, Figure 8, Figure 9, and Figure 10 show the highest values of the three measures - CSI, HSS, and ENT, respectively - as obtained by dichotomizing each variable. The outstanding predictors according to this method are tabulated in Table 7, in order of their (statistically non-significant) predictive strength.

Another important quantity in this method is the value, or the range of values, of the decision threshold (warning/no-warning) for which the highest performance is reached. These quantities are given in the next subsection.

One final comment about this measure-based method is in order. There is some ambiguity regarding the predictive strength of a variable, because that strength may depend on the particular measure being optimized. The reason for this is that different measures gauge different aspects of performance. As such, it is important to select an appropriate measure. It has been shown in (Marzban 1998a) that CSI is pathological in many respects. Indeed, one of its pathologies is evident in Figure 8, where the value of CSI is rather constant for all of the variables; this is related to the "inequitability" of CSI. Inequitability (Gandin and Murphy 1992, Marzban and Lakshmanan, 1998), is defined as the use of an inequitable measure which can cause a forecaster to "hedge" the forecasts. In the context of the finding thresholds that maximize a measure of performance, inequitability can cause the optimal value of the threshold to be the lowest value of the variable itself. As such, severe over- or under-forecasting can occur (see the next subsection). Inequitability is illustrated in Figure 11, where the values of POD, FAR, CSI, and HSS (ENT is not shown) are plotted as a function of the threshold. For such reasons, it is advisable to place less emphasis on the findings that are based on CSI.

v. Results using correlations among predictors

Pairs of variables with high ($\geq$ 0.9) correlation coefficients for both tornadic and non-tornadic circulations are given in Table 8. $R_0[x][y]$ represents the correlation coefficient between x and y, for non-tornadic circulations, and r_1 represents the same quantity for tornadic circulations. The probability that these values of r could be obtained by chance was computed and was found to be zero (to 12 decimal places). Therefore, to a high level of significance, these values of r are statistically significant. Most of these have a high r because they are essentially measuring similar quantities.

d. Summary of Statistical Analysis

Although the question of best predictors is a multifaceted one, and therefore, deserving of a similar multifaceted analysis, for practical purposes it may be necessary to distill the many facets into one. In other words, acknowledging that the there are many contingencies and ambiguities in addressing that question, can one conclude a set of best predictors that is somewhat insensitive to the ambiguities? The answer is in the affirmative, but it is necessary to provide two separate answers: If an extensive and reliable list of best predictors is desired, then the probabilistic method must be adopted, according to which the best predictors for the first three subsets are (in no particular order)

Subset I: 3, 4, 9, 19, 20, 21, 25-27, 52, 53
Subset II: 2, 3, 4
Subset III: 5, 8, 20, 21, 27, 28, 33, 34, 35, 70, 71

These are also listed in Table 9.

If, on the other hand, a small and restricted set of best predictors is desired, then an answer is offered by the best predictors common to all the "linear" methods (in no particular order).

Subset I: 4, 20, 21
Subset II: 1, 9
Subset III: 14, 17, 27, 28, 59

These are also listed in Table 10. The range of values of the decision threshold over which performance is maximized is given in Table 10, but only for the best predictors according to the "linear" methods.

Refer to the Appendix C for the list of the variables and to Appendix A for a description of the best predictors and some other related variables. Also refer to Table 4 for a closer look at the variable threshold values and Table 8 for those variables that are highly correlated (i.e. r_0 and $r_1 > 0.9$).

APPENDIX C [Top]

List of algorithm parameters for each subset of data

Subset I (MDA)

1. Range (km)
2. Base (m)
3. Depth (m)
4. Strength rank
5. Low-altitude diameter (m)
6. Maximum diameter (m)
7. Height of maximum diameter (m)
8. Low-altitude rotational velocity (m/s)
9. Maximum rotational velocity (m/s)
10. Height of maximum rotational velocity (m)
11. Low-altitude shear (m/s/km)
12. Maximum shear (m/s/km)
13. Height of maximum shear (m)
14. Low-altitude gate-to-gate velocity difference (m/s)
15. Maximum gate-to-gate velocity difference (m/s)
16. Height of maximum gate-to-gate velocity difference (m)
17. Core base (m)
18. Core depth (m)
19. Age (min)
20. Strength index (MSI) weighted by average density of integrated layer
21. Strength index (MSIr) “rank”
22. Relative depth (%)
23. Low-altitude convergence (m/s)
24. Mid-altitude convergence (m/s)
25. Vertically-integrated rotational velocity (m/s)
26. Vertically-integrated Shear (m/s/km)
27. Vertically-integrated gate-to-gate velocity difference (m/s)
28. Trend base (m)
29. Trend depth (m)
30. Trend strength rank
31. Trend low-altitude diameter (m)
32. Trend maximum diameter (m)
33. Trend height of maximum diameter (m)
34. Trend low-altitude rotational velocity (m/s)
35. Trend maximum rotational velocity (m/s)
36. Trend height of maximum rotational velocity (m)

37. Trend low-altitude shear (m/s/km)
38. Trend maximum shear (m/s/km)
39. Trend height of maximum shear (m)
40. Trend low-altitude gate-to-gate velocity difference (m/s)
41. Trend maximum gate-to-gate velocity difference (m/s)
42. Trend height of max g-t-g vel difference (m)
43. Trend strength index (MSI) weighted average density of integrated layer
44. Trend strength index (MSIr) “rank”
45. Trend relative depth (%)
46. Trend low-altitude convergence (m/s)
47. Trend mid-altitude convergence (m/s)
48. Trend Vertically-integrated rotational velocity (m/s)
49. Trend Vertically-integrated Shear (m/s/km)
50. Trend Vertically-integrated gate-to-gate velocity difference (m/s)
51. Trend Delta-V slope
52. Integrated Rotational Strength (IRS) index (NWS method-add up 2D values)
53. IRS method - trapezoidal integration divided by depth of integration

Subset II (TDA)

1. Base (m)
2. Depth [DPTH] (m)
3. Low-altitude gate-to-gate velocity difference [LLDV] (m/s)
4. Maximum gate-to-gate velocity difference [MDV] (m/s)
5. Height of maximum gate-to-gate velocity difference (m)
6. Low-altitude shear (m/s/km)
7. Maximum shear (m/s/km)
8. Height of maximum shear (m)
9. Tornado Strength Index (TSI)
10. Trend base (m)
11. Trend depth (m)
12. Trend low-altitude gate-to-gate velocity difference (m/s)
13. Trend maximum gate-to-gate velocity difference (m/s)
14. Trend ht of max gate-to-gate velocity difference (m)
15. Trend low-altitude shear (m/s/km)
16. Trend maximum shear (m/s/km)
17. Trend height of maximum shear (m)
18. Trend Tornado Strength Index (TSI)
19. Range (km)

Subset III (MDA+TDA)

1. Meso range (km)
2. Meso base (m)
3. Meso depth (m)
4. Meso strength rank
5. Meso low-altitude diameter (m)
6. Meso maximum diameter (m)
7. Meso height of maximum diameter (m)
8. Meso low-altitude rotational velocity (m/s)
9. Meso maximum rotational velocity (m/s)
10. Meso height of maximum rotational velocity (m)
11. Meso low-altitude shear (m/s/km)
12. Meso maximum shear (m/s/km)
13. Meso height of maximum shear (m)
14. Meso low-altitude gate-to-gate velocity difference (m/s)
15. Meso maximum gate-to-gate velocity difference (m/s)
16. Meso height of maximum gate-to-gate velocity difference (m)
17. Meso core base (m)
18. Meso core depth (m)
19. Meso age (min)
20. Meso strength index (MSI) weighted by average density of integrated layer
21. Meso strength index (MSIr) “rank”
22. Meso relative depth (%)
23. Meso low-altitude convergence (m/s)
24. Meso mid-altitude convergence (m/s)
25. TVS base (m)
26. TVS depth [DPTH] (m)
27. TVS low-altitude gate-to-gate velocity difference [LLDV] (m/s)
28. TVS maximum gate-to-gate velocity difference [MDV] (m/s)
29. TVS height of maximum gate-to-gate velocity difference (m)
30. TVS low-altitude shear (m/s/km)
31. TVS maximum shear (m/s/km)
32. TVS height of maximum shear (m)
33. Meso Vertically-integrated rotational velocity (m/s)
34. Meso Vertically-integrated Shear (m/s/km)
35. Meso Vertically-integrated gate-to-gate velocity difference (m/s)
36. Meso trend base (m)
37. Meso trend depth (m)
38. Meso trend strength rank
39. Meso trend low-altitude diameter (m)
40. Meso trend maximum diameter (m)

41. Meso trend height of maximum diameter (m)
42. Meso trend low-altitude rotational velocity (m/s)
43. Meso trend maximum rotational velocity (m/s)
44. Meso trend height of maximum rotational velocity (m)
45. Meso trend low-altitude shear (m/s/km)
46. Meso trend maximum shear (m/s/km)
47. Meso trend height of maximum shear (m)
48. Meso trend low-altitude gate-to-gate velocity difference (m/s)
49. Meso trend maximum gate-to-gate velocity difference (m/s)
50. Meso trend height of max g-t-g vel difference (m)
51. Meso trend strength index (MSI) weighted by average density of integrated layer
52. Meso trend strength index (MSIr) “rank”
53. Meso trend relative depth (%)
54. Meso trend low-altitude convergence (m/s)
55. Meso trend mid-altitude convergence (m/s)
56. Meso trend Vertically-integrated rotational velocity (m/s)
57. Meso trend Vertically-integrated Shear (m/s/km)
58. Meso trend Vertically-integrated gate-to-gate velocity difference (m/s)
59.Tornado Strength Index (TSI)
60. TVS trend base (m)
61. TVS trend depth (m)
62. TVS trend low-altitude gate-to-gate velocity difference (m/s)
63. TVS trend maximum gate-to-gate velocity difference (m/s)
64. TVS trend height of maximum gate-to-gate velocity difference (m)
65. TVS trend low-altitude shear (m/s/km)
66. TVS trend maximum shear (m/s/km)
67. TVS trend height of maximum shear (m)
68. TVS trend Tornado Strength Index (TSI)
69. Meso trend Delta-V slope
70. Meso Integrated Rotational Strength (IRS) index (NWS method-add up 2D values)
71. Meso IRS (MSI method-trapezoidal integration divided by depth of integration)

Subsets IV, V, and VI are not shown.

APPENDIX D [Top]

Verification Measure Formulae

In the following, the subscripts "0" and "1" will refer to nontornadic and tornadic circulations, respectively. The performance of a forecaster can be tabulated in terms of a contingency table, defined as

$$\text{C}-\text{table} = \begin{pmatrix} C_1 & C_2 \\ C_3 & C_4 \end{pmatrix} = \begin{pmatrix} \#\text{ of 0's predicted as 0} & \#\text{ of 0's predicted as 1} \\ \#\text{ of 1's predicted as 0} & \#\text{ of 1's predicted as 1} \end{pmatrix},$$

$$\begin{pmatrix} . & \text{false alarms} \\ \text{misses} & \text{hits} \end{pmatrix}.$$

The total number of nontornadic circulations is given by $N_0 = C_1 + C_2$, that of tornadic circulations is $N_1 = C_3 + C_4$, and the total sample size is $\text{N} = \text{N}_0 + \text{N}_1$.

Two common quantities, Probability of Detection (POD) and False Alarm Ratio (FAR), are easily calculated as

$$\text{POD} = \frac{C_4}{C_3 + C_4}, \quad \text{FAR} = \frac{C_2}{C_2 + C_4}.$$

Similarly, the three measures, the Critical Success Index (CSI), the Heidke Skill Statistic (HSS), and the Entropy (ENT) (also known as the Likelihood Ratio Chi-square) can be written as

$$\text{CSI} = \frac{\text{C}_4}{\text{C}_2 + \text{C}_3 + \text{C}_4},$$

$$\text{HSS} = \frac{2\left(\text{C}_1\text{C}_4 - \text{C}_2\text{C}_3\right)}{\text{N}_0\left(\text{C}_2 + \text{C}_4\right) + \text{N}_1\left(\text{C}_1 + \text{C}_3\right)},$$

$$\text{LRC} = -\sum_{i=1}^{4} C_i \log \frac{E_i}{C_i},$$

where C_i and E_i are the contingency table and its (biased) expected value based on pure chance (i.e., guessing), respectively, with the latter computed as

$$\text{E} = \frac{1}{\text{N}} \begin{pmatrix} N_0\left(C_1 + C_3\right) & N_0\left(C_2 + C_4\right) \\ N_1\left(C_1 + C_3\right) & N_1\left(C_2 + C_4\right) \end{pmatrix}.$$

Recall that C_1 and C_4 are the number of correctly classified nontornados and tornados, respectively, and C_2 and C_3 are the number of incorrectly classified nontornados and tornados, respectively.

For further details, consult the on-line articles at http://www.nhn.ou.edu/~marzban/.

TABLES AND FIGURES

Table 1. WSR-88D data cases used for the statistical analysis of the NSSL MDA and TDA.

Radar Site	Date	# Tornadoes	Storm Type
Melbourne, FL	3/25/92	0	supercells
Norman, OK	3/28/92	0	“null” case
Norman, OK	5/11/92	22	supercells
Norman, OK	9/2/92	1	supercell
Sterling, VA	4/16/93	7	mini supercells
Dodge City, KS	5/5/93	11	supercells
Dodge City, KS	5/7/93	9	supercells
Dodge City, KS	6/3/93	0	“null” case
Houston, TX	11/16/93	9	supercells (ascending mesocyclone development)
Dodge City, KS	4/9/94	6	supercells
Houston, TX	4/15/94	1	supercells
St. Louis, MO	4/15/94	8	bowing squall line tornadoes
Oklahoma City, OK	4/27/94	0	“null” case
Sterling, VA	4/30/94	3	low-topped supercells
Tulsa, OK	5/6/94	3	supercells
Tulsa, OK	5/7/94	0	“null” case
Amarillo, TX	5/28/94	1	supercell
Lubbock, TX	6/9/94	0	“null” case
Memphis, TN	6/9/94	4	bowing squall line tornadoes
Melbourne, FL	11/15/94	6	Tropical cyclone mesos
Memphis, TN	11/27/94	7	supercells
Phoenix, AZ	2/13/95	1	mini supercell
Fort Worth, TX	4/19/95	18	supercells
Fort Worth, TX	5/4/95	0	“null” case
Fort Worth, TX	5/5/95	0	supercells
Fort Worth, TX	5/7/95	12	supercells
Goodland, KS	5/12/95	5	supercell
Dodge City, KS	5/16/95	2	supercells
Dodge City, KS	5/17/95	3	supercells
Amarillo, TX	5/22/95	8	supercell

Oklahoma City, OK	5/23/95	0	“null” case
Des Moines, IA	5/27/95	6	supercells
Lubbock TX	6/2/95	9	supercells
Pueblo, CO	6/22/95	1	mini supercell
Minneapolis, MN	7/21/95	12	supercells
Minneapolis, MN	8/9/95	0	“null” case
Birmingham, AL	3/18/96	6	supercells
Denver, CO	5/22/96	1	supercells
Detroit, MI	6/22/96	3	supercells
Sterling, VA	7/12/96	6	tropical-cyclone mesos
Minneapolis, MN	10/26/96	9	low-topped supercells
Sacramento, CA	12/12/96	1	mini supercells
Amarillo, TX	6/11/97	6	supercells
TOTAL		207	

Table 2. Optimized adaptable parameter values and TDA performance for various convective data sets. The two right-hand columns are based on the composite data set.

Optimized (CSI and FAR) Parameters and TDA Performance	Data Set			Minimized FAR Parameter Set	Old TVS Algorithm Performance
	Composite (Default)	Isolated	SqLine/ Other		
DPTH (km)	1.5	3.1	1.6	5.0	NA
LLDV (m s^{-1})	25	27	27	56	NA
MDV (m s^{-1})	36	30	27	74	NA
POD (%)	32	43	18	2	7
FAR (%)	61	44	77	8	8
CSI[(5)] (%)	21	32	11	2	7

Table 3. The sample sizes, the a-priori probabilities, and the number of attributes. The total sample size is N, the number of non-tornadoes is N_0, the number of tornadoes is N_1, and the *a-priori* probability (i.e. climatological, and *prior* to additional statistical analysis) of tornado is $p_1 * 10^2$.

Subset	N	N_0	N_1	$p_1 * 10^2$	No. Of Attributes
I	19841	19222	619	3%	53
Ia*	1968	1764	204	10.4%	53
II	6756	6402	354	5%	19
IIa**	126	118	8	6.3%	19
III	1198	822	376	31%	71
IV	1802	1645	157	9%	67
V	1411	1276	135	9%	33
VI	493	307	186	38%	85

*Circulations detected by a MDA rank of five or greater, only
**Circulations detected by a TDA Default, only

Table 4. An interactive table summarizing the "best predictors" from the statistical analyses for subsets I, II, and III. Within this table are links to algorithm parameter descriptions from Appendix A, probability plot figures, and decision threshold figures [based on Heidke Skill Statistic (HSS)]. The decision thresholds are the range of value at which special warning consideration should be given if value are at or above this threshold. The two exceptions are indicated by the *, in which the special consideration should be given to values at or *below* the threshold. The variables marked with ** are only available via the WDSS or WATADS.

Subset	Variable	Name (from Appendix A)	Probability and Threshold Plots	HSS threshold (metric units)	HSS threshold (english units)
I MDA only	3	MDA Depth	Fig. PT-1	10-11 km	33-36 kft
	4**	MDA Strength Rank	Fig. PT-2	5	5
	9	MDA Max Rotational Velocity	Fig. PT-3	18-22 ms^{-1}	35-43 kts
	19	MDA Age	Fig. PT-4	30-60 min	30-60 min
	20**	MDA Meso Strength Index (MSI)	Fig. PT-5	3500-4000	3500-4000
II TDA only	1*	TDA Base	Fig. PT-6	2.8-3.3 km	9.2-10.8 kft
	2	TDA Depth [DPTH]	Fig. PT-7	6.8-7.3 km	22.3-24.0 kft
	3	TDA low-alt. Gate-to-gate delta-V [LLDV]	Fig. PT-8	27-32 ms^{-1}	52-62 kts
	4	TDA max gate-to-gate delta-V [MDV]	Fig. PT-9	31-38 ms^{-1}	60-74 kts
III MDA and TDA	5*	MDA low-alt. Diameter	Fig. PT-10	6.7 km	3.6 Nmi
	8	MDA low-alt. Rot. Vel.	Fig. PT-11	19-24 ms^{-1}	37-47 kts
	14	MDA low-alt. gate-to-gate delta-V	Fig. PT-12	32-36 ms^{-1}	62-70 kts
	17*	MDA Core Base	Fig. PT-13	2.4-2.6 km	7.9-8.5 kft
	27	TDA low-alt. gate-to-gate delta-V [LLDV}	Fig. PT-14	35-42 ms^{-1}	68-81 kts
	28	TDA max gate-to-gate delta-V [MDV]	Fig. PT-15	42-52 ms^{-1}	81-101 kts

Table 5. A classification of the predictors according to the posterior probability method. See Appendix C for the list of the variables.

	Predictive Strength	Predictors (see Appendix C)
Subset I	Good	3,4,9,19,20,21,25-27,52,53
	Fair	2,8,11,12,14,15,18,22,23,30,33,34-37,41,43,44,48-51
	Poor	1,5,6,7,10,13,16,17,24,28,29,31,32,38-40,42,45-47
Subset II	Good	2,3,4
	Fair	1,5-13,15,16,18
	Poor	14,17,19
Subset III	Good	5,8,20,21,27,28,33,34,35,70,71
	Fair	2,4,9-17,19,22-25,29-32,44-47,59,60,62,63,65-69
	Poor	1,3,6,7,18,26,36,37-43,48-58,61,64

Table 6. The best predictors according to the correlation-based method. Variables enclosed in parentheses have statistically equivalent predictive strengths. See Appendix C for the list of the variables.

Subset	Best Predictors
I	(20,27,53),(4,8,14,21,25)
II	1,3,(4,5,8,9)
III	(14,27),(11,30,59),(8,17,20,28,34)

Table 7. The “Top 5" predictors according to the measure-based method. See Appendix C for the list of the variables.

	Best Predictors		
Subset	CSI	HSS	ENT
I	20,14,4,53,15	53,20,14,4,21	4,8,25,21,20
II	3,2,9,4,7	3,2,9,4,1	1,9,10,8,5
III	59,23,27,54,11	59,14,17,27,28	59,27,14,17,28

Table 8. Correlation coefficients for tornadic (1) and non-tornadic (0) circulations for the highly correlated variables in the six subsets. The corresponding pair of variables may be considered statistically equivalent.

Subset	Correlation Coefficients	
I	r_0[17][2]=0.940, r_1=0.90	r_0[50][41]=0.919, r_1=0.906
	r_0[48][35]=0.923, r_1=0.922	r_0[50][48]=0.911, r_1=0.912
	r_0[48][43]=0.911, r_1=0.935	r_0[53][25]=0.948, r_1=0.950
II	r_0[8][5]=0.973, r_1=0.963	r_0[17][4]=0.981, r_1=0.967
III	r_0[32][29]=0.973, r_1=0.955	r_0[71][33]=0.937, r_1=0.938
	r_0[67][64]=0.975, r_1=0.940	

Table 9. The variable considered "best predictors" common to the probabilistic method. See Appendix C for the list of the variables.

Subset	Variable	Name
I	3	MDA Depth
	4	MDA Strength Rank
	9	MDA Max Rotational Velocity
	19	MDA Age
	20	MDA MSI
	21	MDA MSI "rank"
	25	MDA Vertically-integrated rotational velocity
	26	MDA Vertically-integrated shear
	27	MDA Vertically-integrated gate-to-gate delta-V
	52	MDA Integrated Rotational Strength (IRS) Index
	53	MDA IRS Index (divided by depth of integration)
II	2	TDA Depth [DPTH]
	3	TDA low-altitude gate-to-gate delta-V [LLDV]
	4	TDA Maximum gate-to-gate delta-V [MDV]
III	5	MDA low-altitude diameter
	8	MDA low-altitude rotational velocity
	20	MDA MSI
	21	MDA MSI "rank"
	27	TDA low-altitude gate-to-gate delta-V [LLDV]
	28	TDA Maximum gate-to-gate delta-V [MDV]
	33	MDA Vertically-integrated rotational velocity
	34	MDA Vertically-integrated shear
	35	MDA Vertically-integrated gate-to-gate delta-V
	70	MDA Integrated Rotational Strength (IRS) Index
	71	MDA IRS Index (divided by depth of integration)

Table 10. The variable considered "best predictors" common to all the "linear" methods. The range of thresholds over which performance is maximized is also shown. The * symbol indicates that the maximum of CSI occurs at the lowest value of the variable. See Appendix C for the list of the variables.

Subset	Variable	Name	CSI	HSS	ENT
I	4	MDA Strength Rank	4-5	4-5	1-2
	20	MDA MSI	3000-4000	3500-4000	1600-2200
	21	MDA MSI "rank"	3-5	4-5	1-3
II	1	TDA Base	1000-1500	650-1500 m	1900-2500 m
	9	Tornado Strength Index (TSI)	3000-6500	5000-7500	2500-3500
III	14	MDA LL gate-to-gate delta-V	20-26 ms^{-1}*	29-40 ms^{-1}	24-36 ms^{-1}
	17	MDA Core base	2300-3000 m*	1500-2500 m	2400-2700 m
	27	TDA LL gate-to-gate delta-V [LLDV]	23-30 ms^{-1}*	33-42 ms^{-1}	27-42 ms^{-1}
	28	TDA max gate-to-gate delta-V [MDV]	24-37 ms^{-1}*	44-50 ms^{-1}	42-47 ms^{-1}

Figure PT-1. MDA Depth (m): a) Probability plot. In red (solid line) is the probability from Eq. (1) in Appendix B. The dashed (dotted) line with the 1's (0's) is the probability density of tornadic (non-tornadic) detections; b) Decision Threshold plot. POD is in red, FAR is in green, and HSS*10 is in black. For subset I (MDA) only.

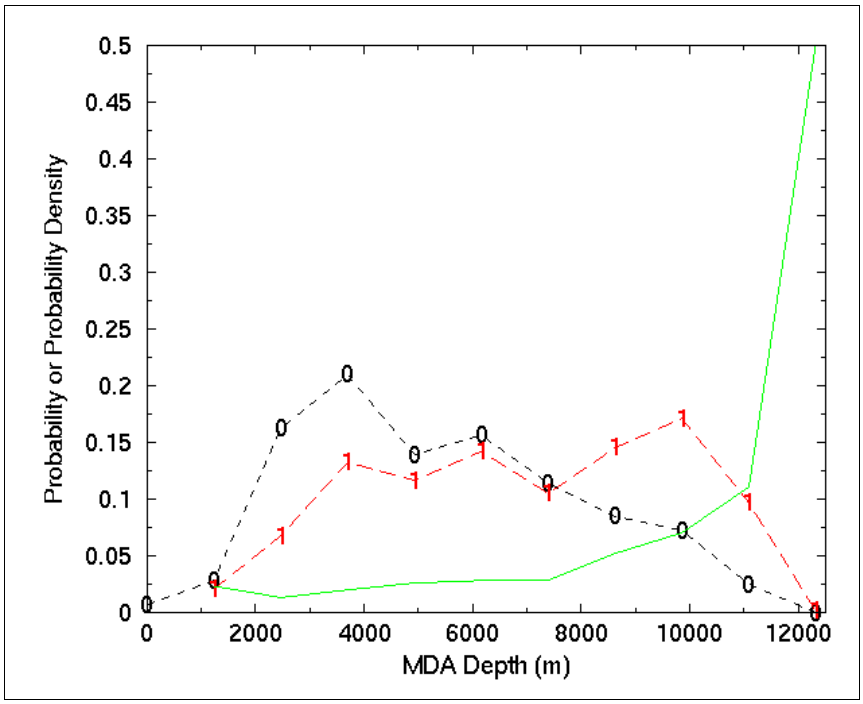

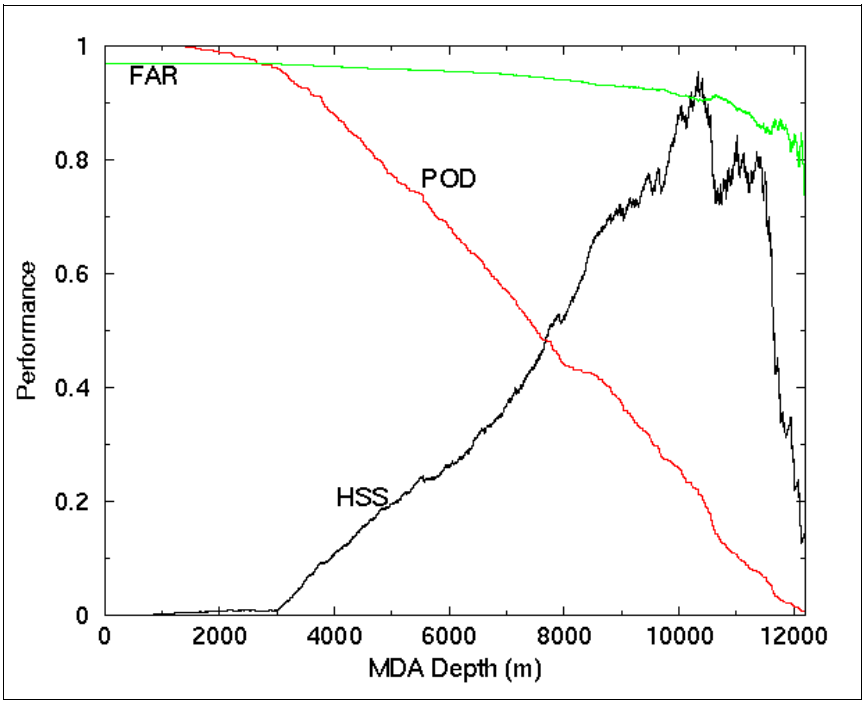

Figure PT-2. MDA Strength Rank: a) Probability plot. In red (solid line) is the probability from Eq. (1) in Appendix B. The dashed (dotted) line with the 1's (0's) is the probability density of tornadic (non-tornadic) detections; b) Decision Threshold plot. POD is in red, FAR is in green, and HSS*10 is in black. For subset I (MDA) only.

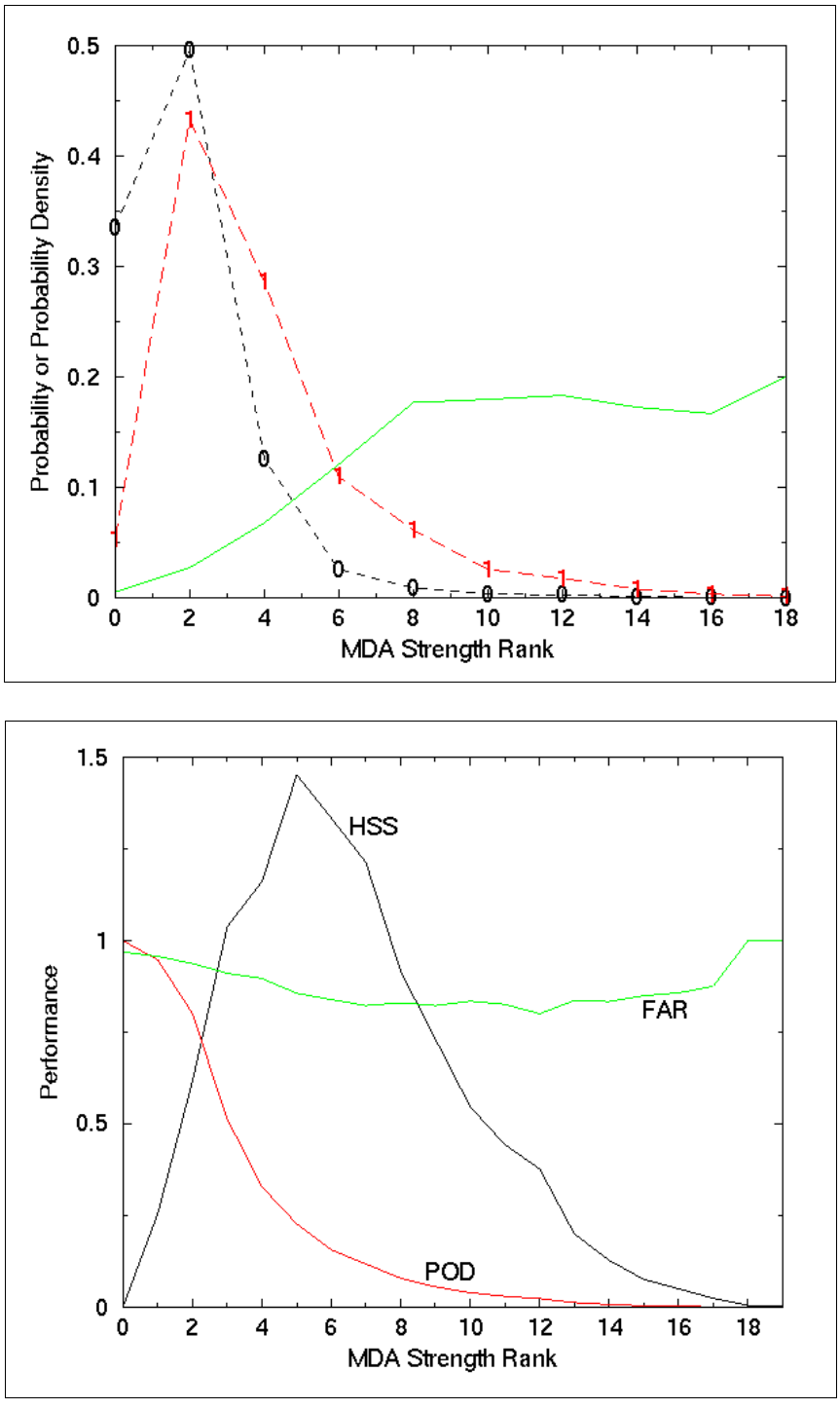

Figure PT-3. MDA Maximum Rotational Velocity (m/s): a) Probability plot. In red (solid line) is the probability from Eq. (1) in Appendix B. The dashed (dotted) line with the 1's (0's) is the probability density of tornadic (non-tornadic) detections; b) Decision Threshold plot. POD is in red, FAR is in green, and HSS*10 is in black. For subset I (MDA) only.

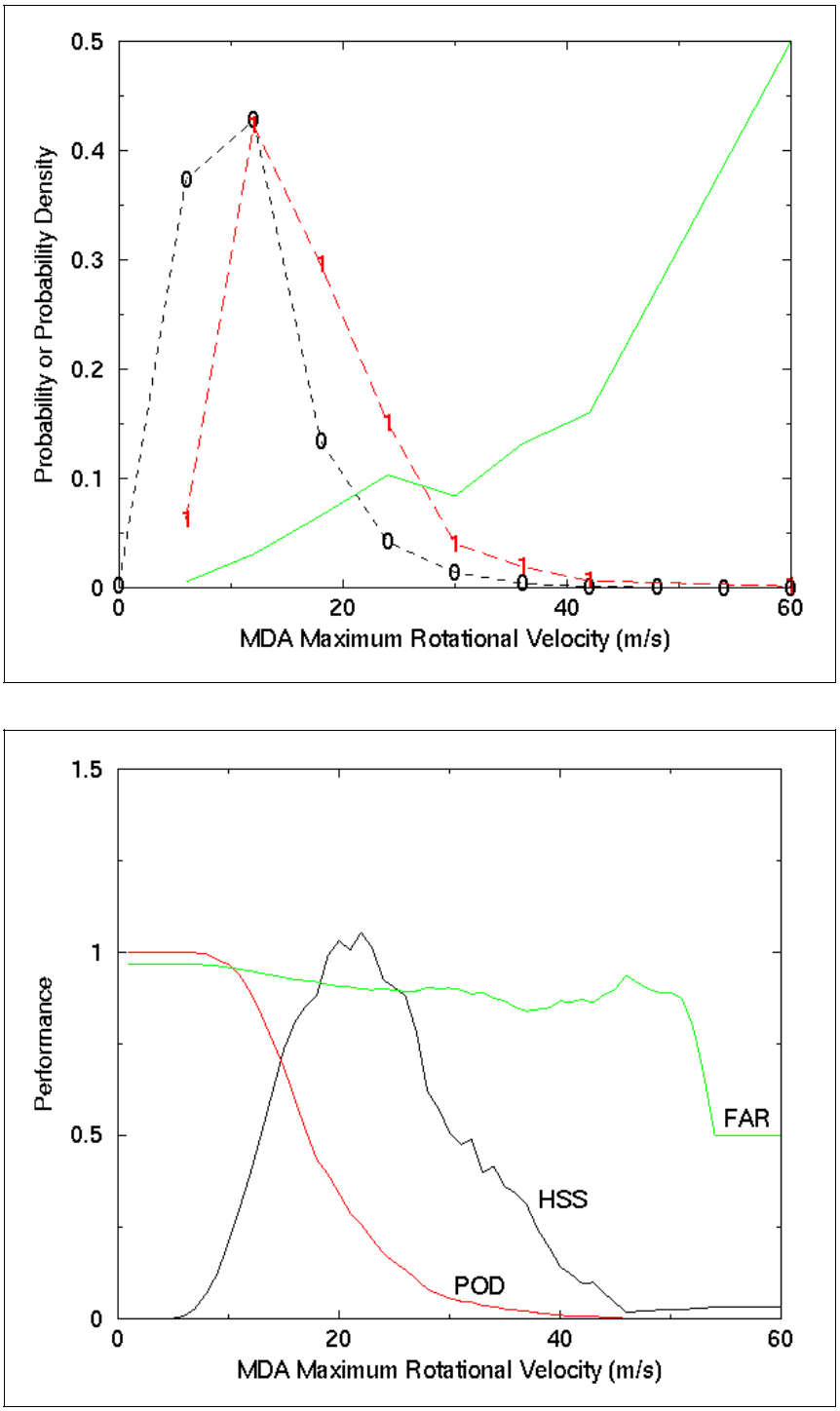

Figure PT-4. MDA Age (minutes): a) Probability plot. In red (solid line) is the probability from Eq. (1) in Appendix B. The dashed (dotted) line with the 1's (0's) is the probability density of tornadic (non-tornadic) detections; b) Decision Threshold plot. POD is in red, FAR is in green, and HSS*10 is in black. For subset I (MDA) only.

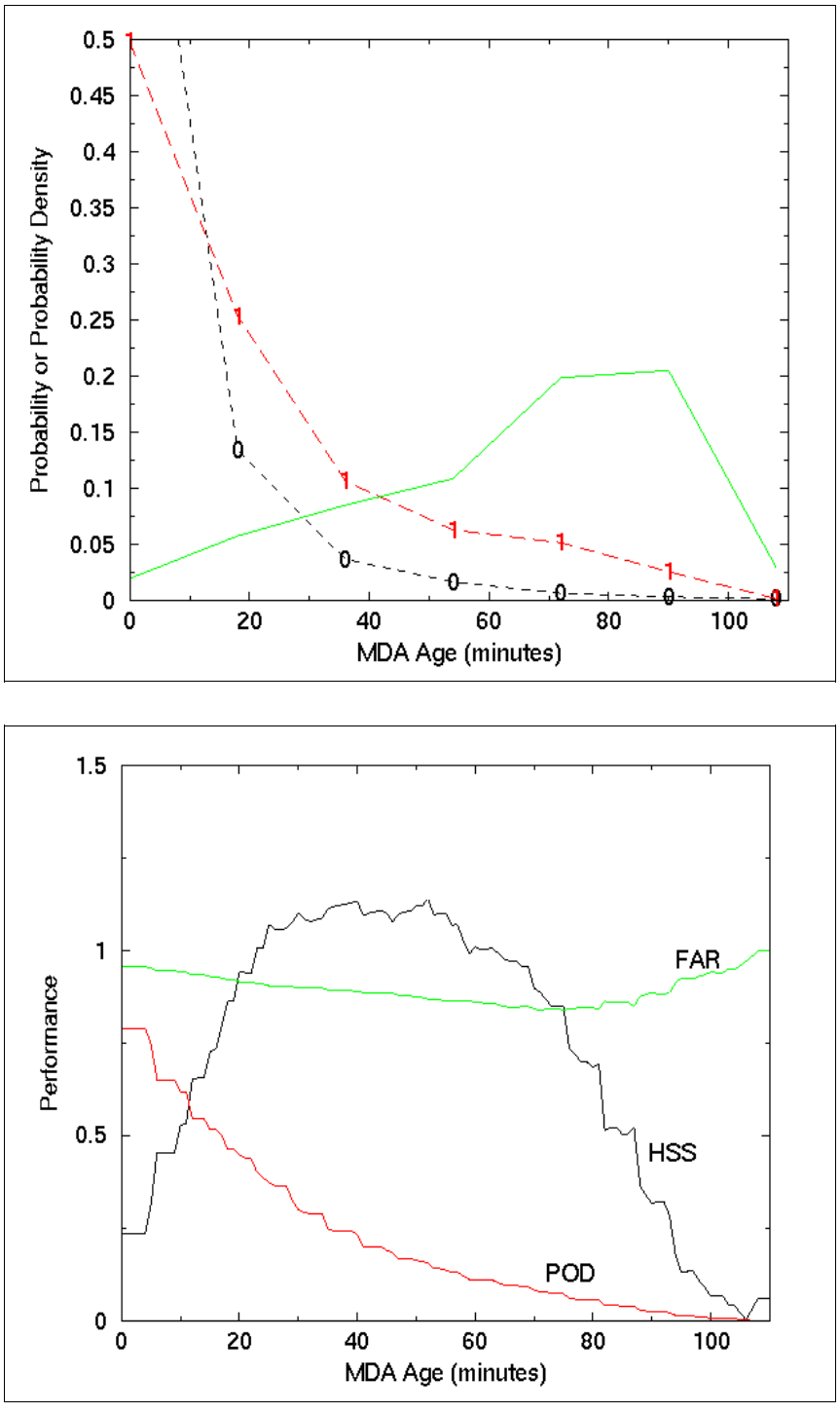

Figure PT-5. MDA Mesocyclone Strength Index (MSI): a) Probability plot. In red (solid line) is the probability from Eq. (1) in Appendix B. The dashed (dotted) line with the 1's (0's) is the probability density of tornadic (non-tornadic) detections; b) Decision Threshold plot. POD is in red, FAR is in green, and HSS*10 is in black. For subset I (MDA) only.

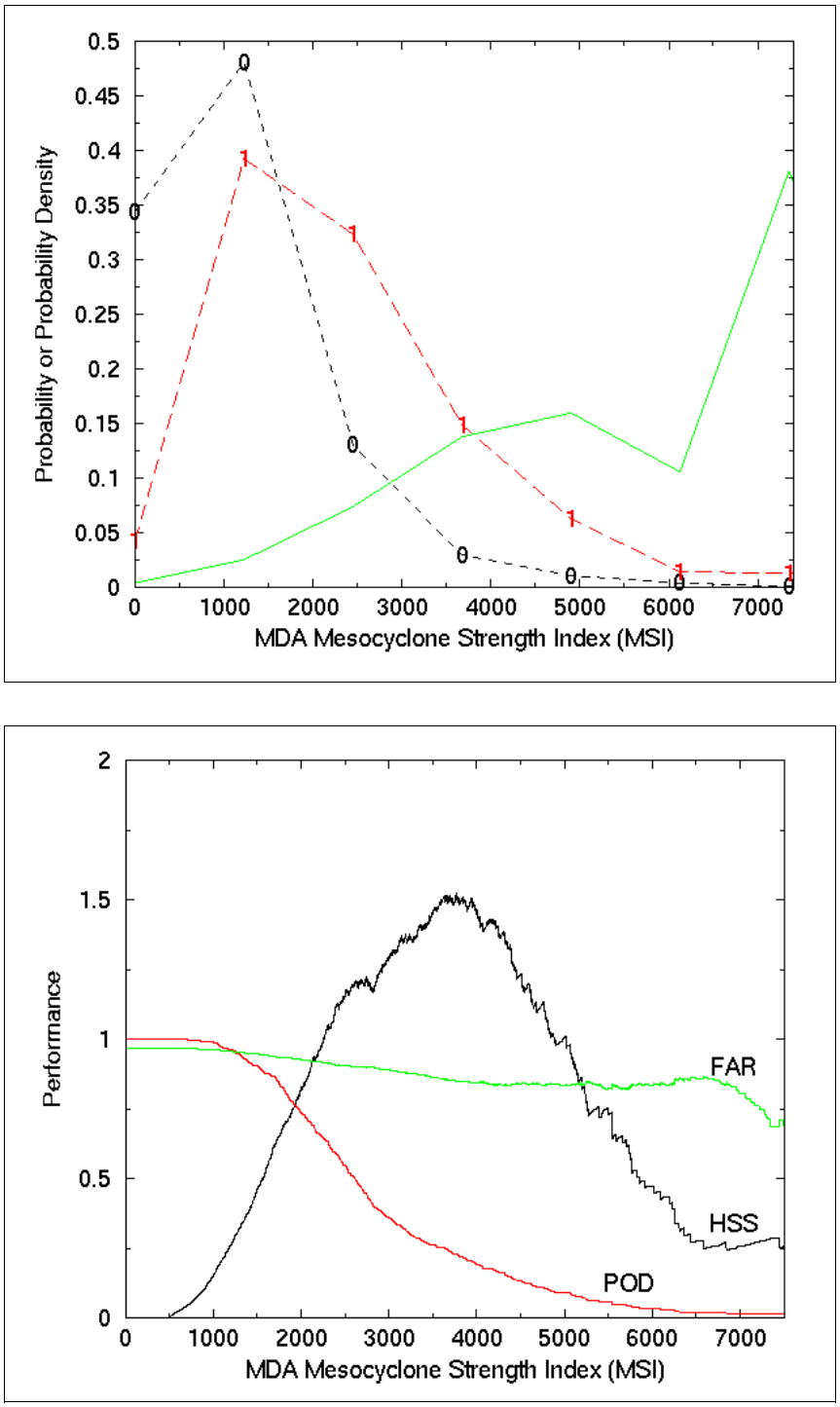

Figure PT-6. TDA Base (m AGL): a) Probability plot. In red (solid line) is the probability from Eq. (1) in Appendix B. The dashed (dotted) line with the 1's (0's) is the probability density of tornadic (non-tornadic) detections; b) Decision Threshold plot. POD is in red, FAR is in green, and HSS*10 is in black. For subset II (TDA) only.

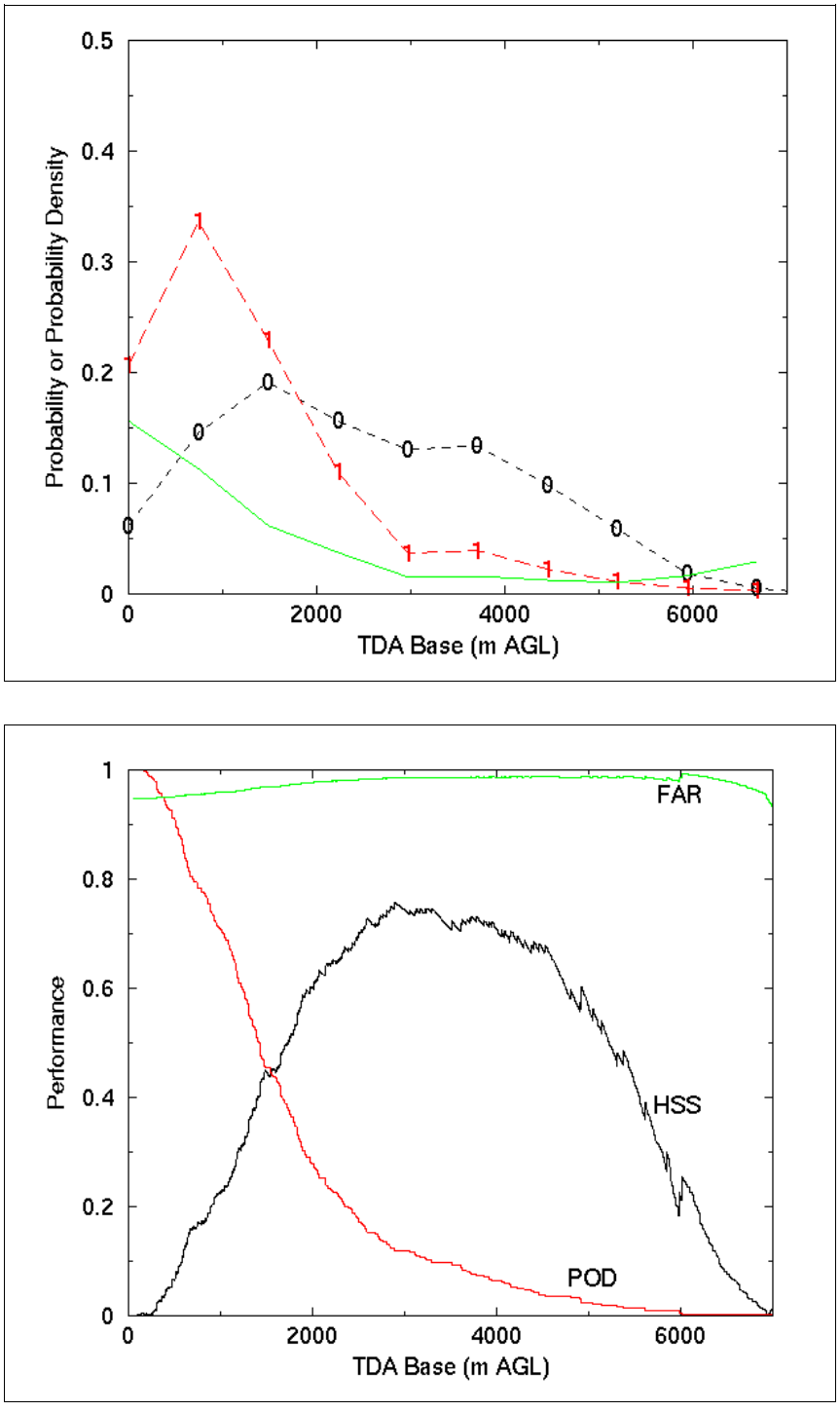

Figure PT-7. TDA Depth [DPTH] (m): a) Probability plot. In green (solid line) is the probability from Eq. (1) in Appendix B. The dashed (dotted) line with the 1's (0's) is the probability density of tornadic (non-tornadic) detections; b) Decision Threshold plot. POD is in red, FAR is in green, and HSS*10 is in black. For subset II (TDA) only.

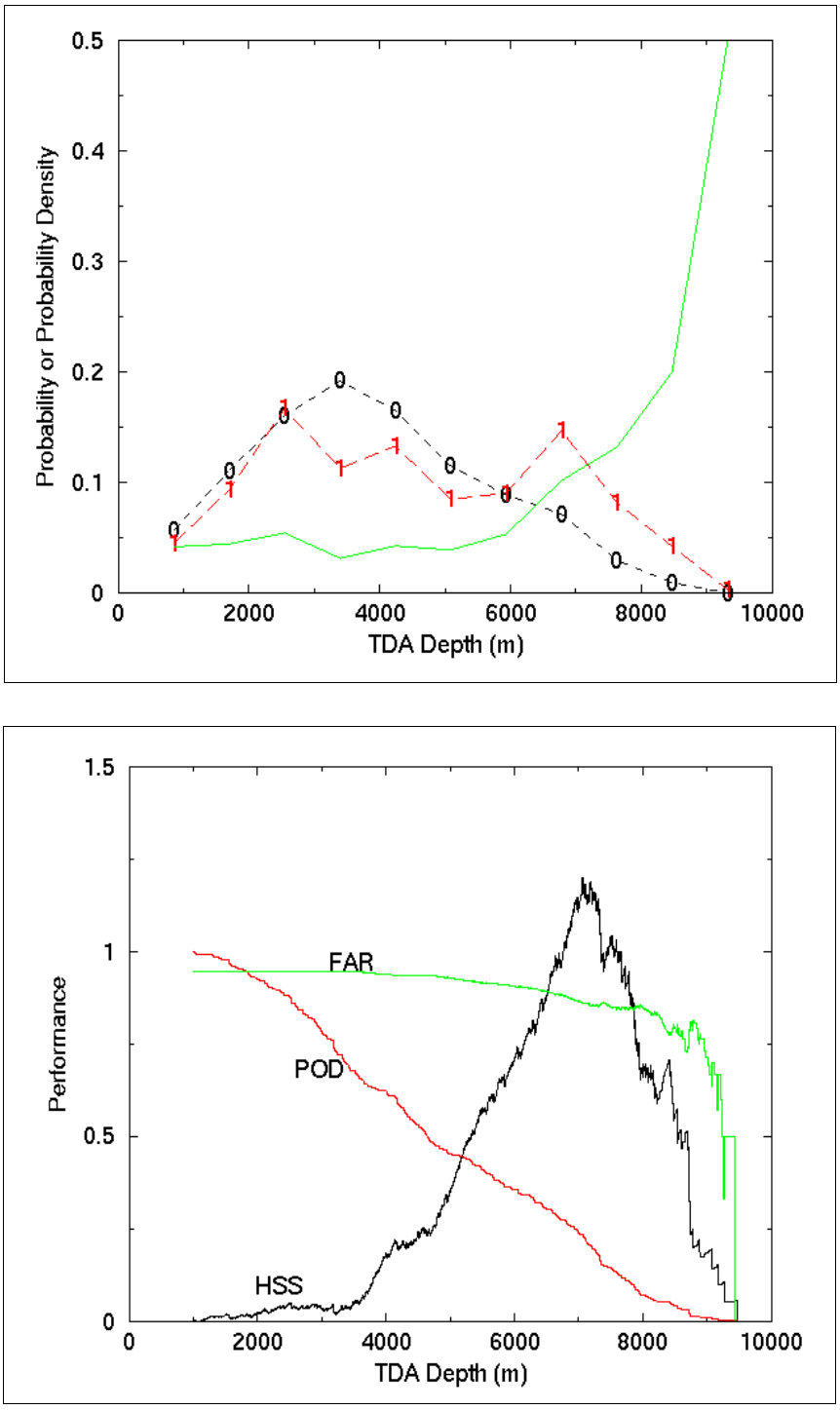

Figure PT-8. TDA low-altitude Gate-to-gate delta-V [LLDV] (m/s): a) Probability plot. In red (solid line) is the probability from Eq. (1) in Appendix B. The dashed (dotted) line with the 1's (0's) is the probability density of tornadic (non-tornadic) detections; b) Decision Threshold plot. POD is in red, FAR is in green, and HSS*10 is in black. For subset II (TDA) only.

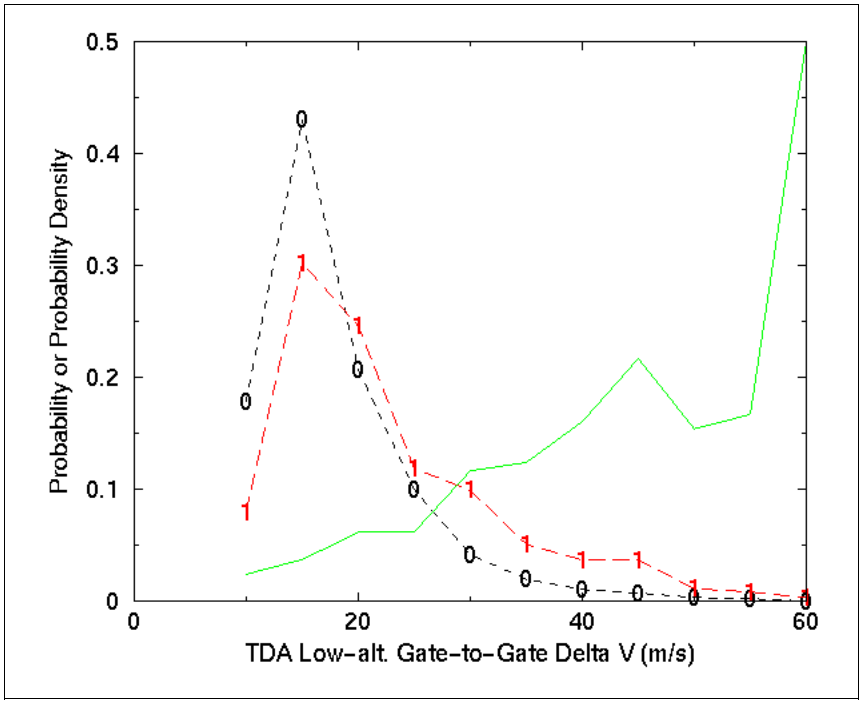

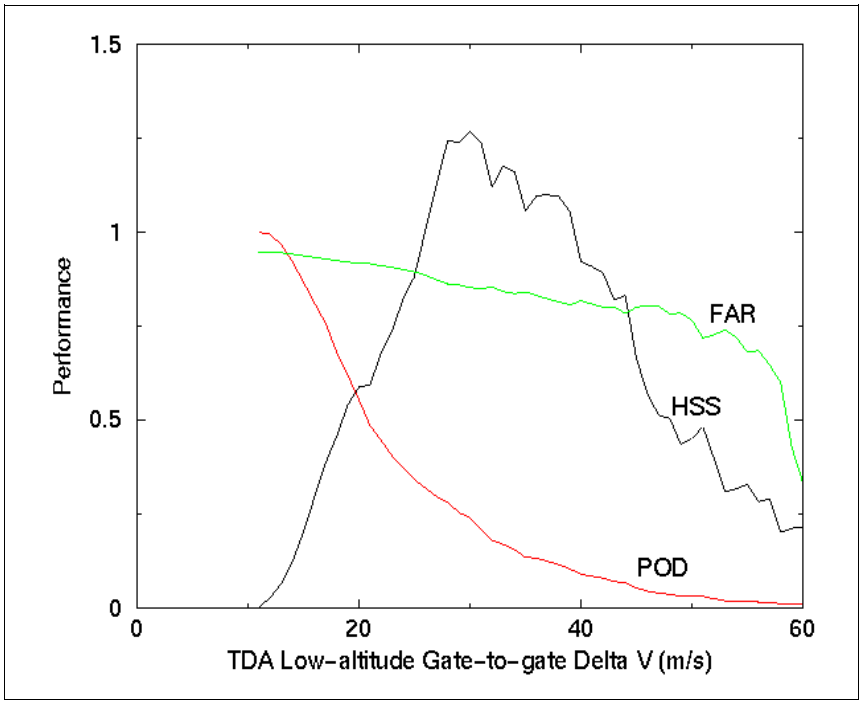

Figure PT-9. TDA maximum gate-to-gate delta-V [MDV] (m/s): a) Probability plot. In red (solid line) is the probability from Eq. (1) in Appendix B. The dashed (dotted) line with the 1's (0's) is the probability density of tornadic (non-tornadic) detections; b) Decision Threshold plot. POD is in red, FAR is in green, and HSS*10 is in black. For subset II (TDA) only.

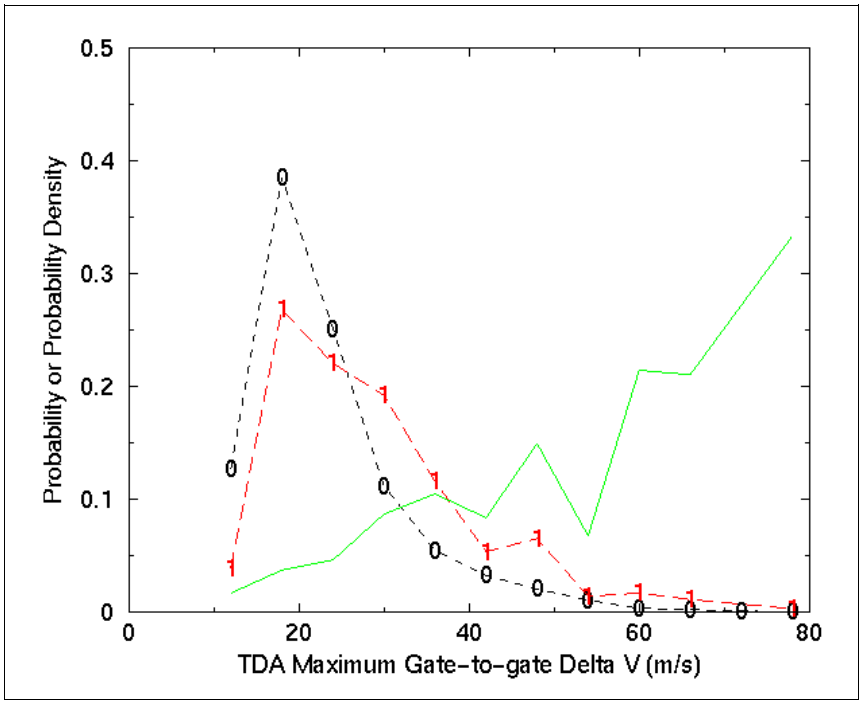

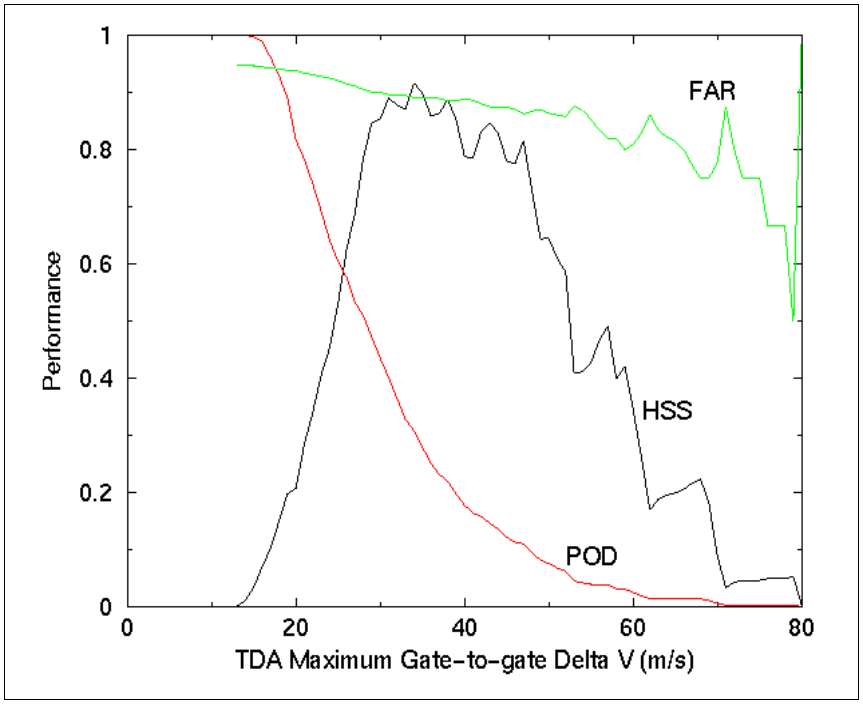

Figure PT-10. MDA low-altitude Diameter (m): a) Probability plot. In red (solid line) is the probability from Eq. (1) in Appendix B. The dashed (dotted) line with the 1's (0's) is the probability density of tornadic (non-tornadic) detections; b) Decision Threshold plot. POD is in red, FAR is in green, and HSS*10 is in black. For subset III (MDA+TDA) only.

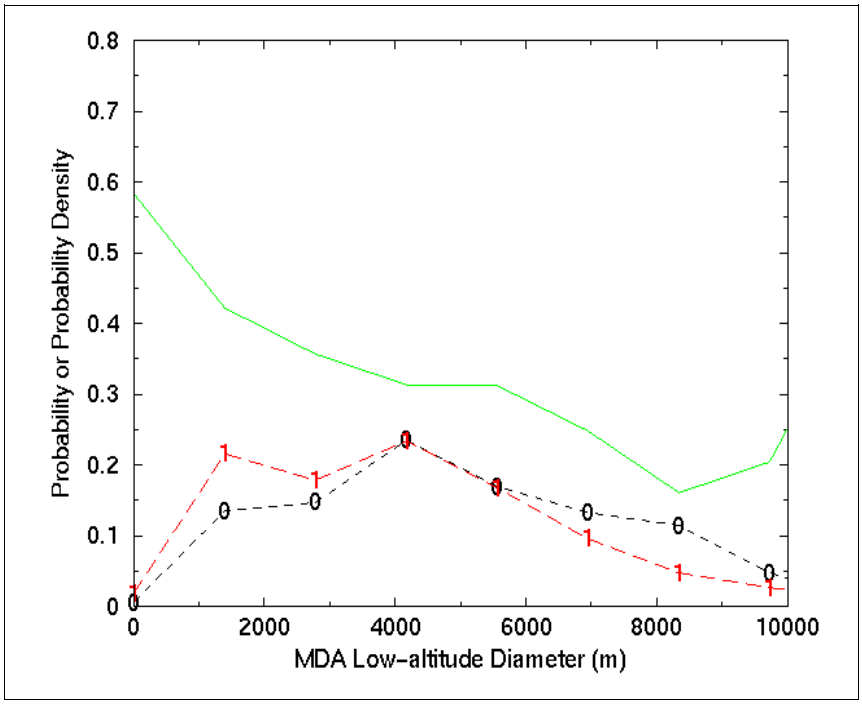

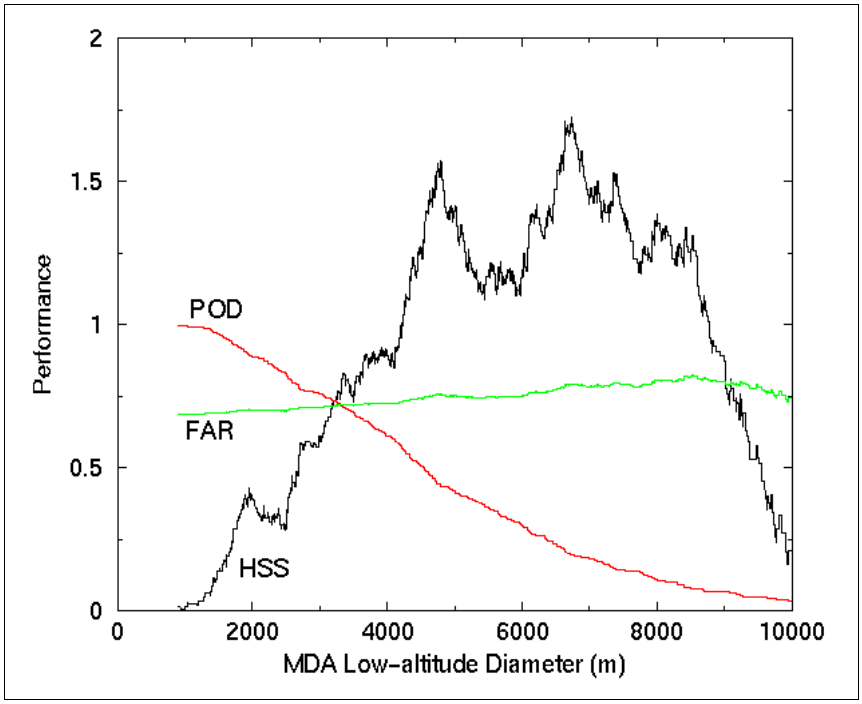

Figure PT-11. MDA low-altitude rotational velocity (m/s): a) Probability plot. In red (solid line) is the probability from Eq. (1) in Appendix B. The dashed (dotted) line with the 1's (0's) is the probability density of tornadic (non-tornadic) detections; b) Decision Threshold plot. POD is in red, FAR is in green, and HSS*10 is in black. For subset III (MDA+TDA) only.

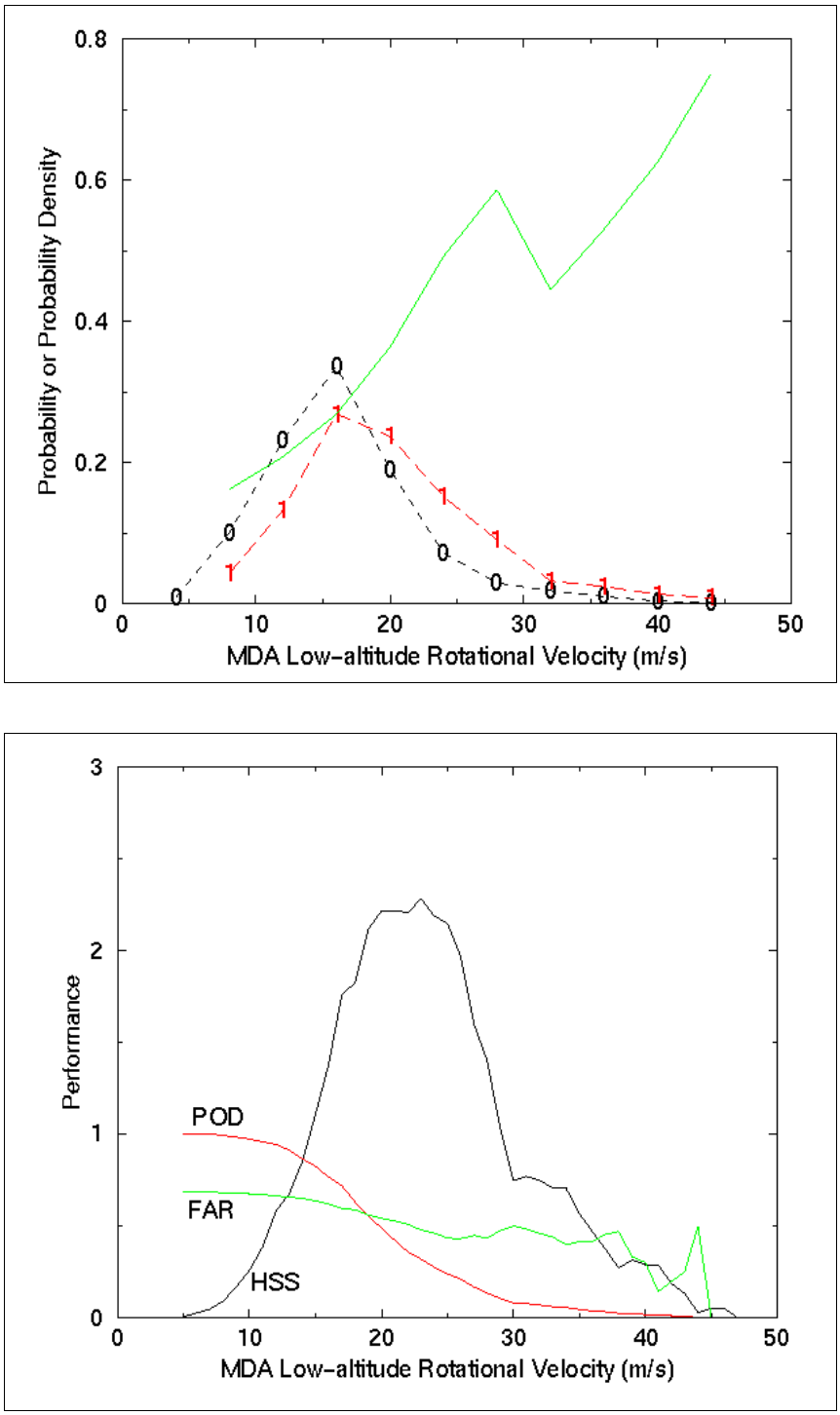

Figure PT-12. MDA low-altitude gate-to-gate delta-V (m/s): a) Probability plot. In red (solid line) is the probability from Eq. (1) in Appendix B. The dashed (dotted) line with the 1's (0's) is the probability density of tornadic (non-tornadic) detections; b) Decision Threshold plot. POD is in red, FAR is in green, and HSS*10 is in black. For subset III (MDA+TDA) only.

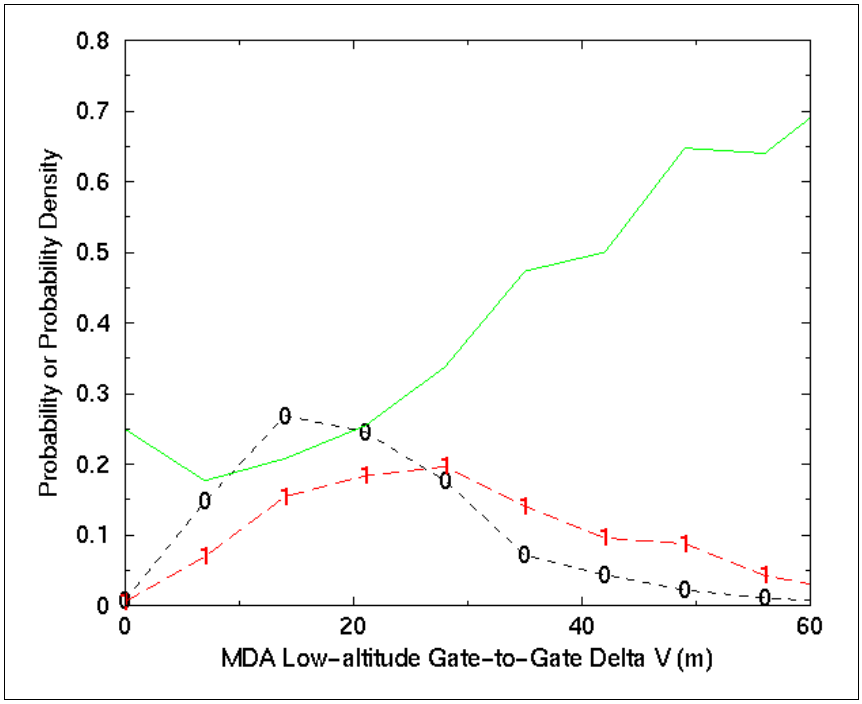

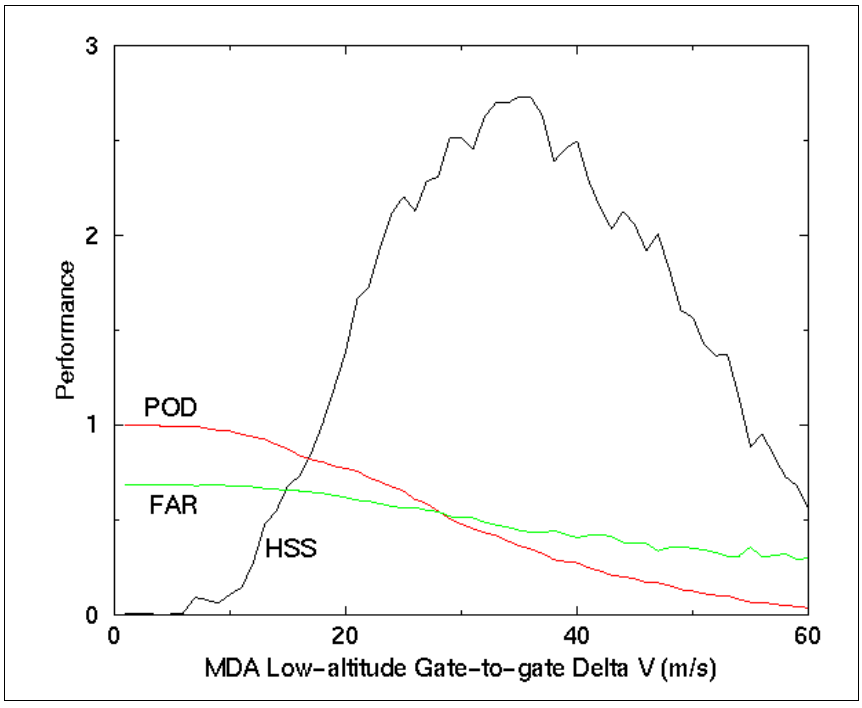

Figure PT-13. MDA Core Base (m AGL): a) Probability plot. In red (solid line) is the probability from Eq. (1) in Appendix B. The dashed (dotted) line with the 1's (0's) is the probability density of tornadic (non-tornadic) detections; b) Decision Threshold plot. POD is in red, FAR is in green, and HSS*10 is in black. For subset III (MDA+TDA) only.

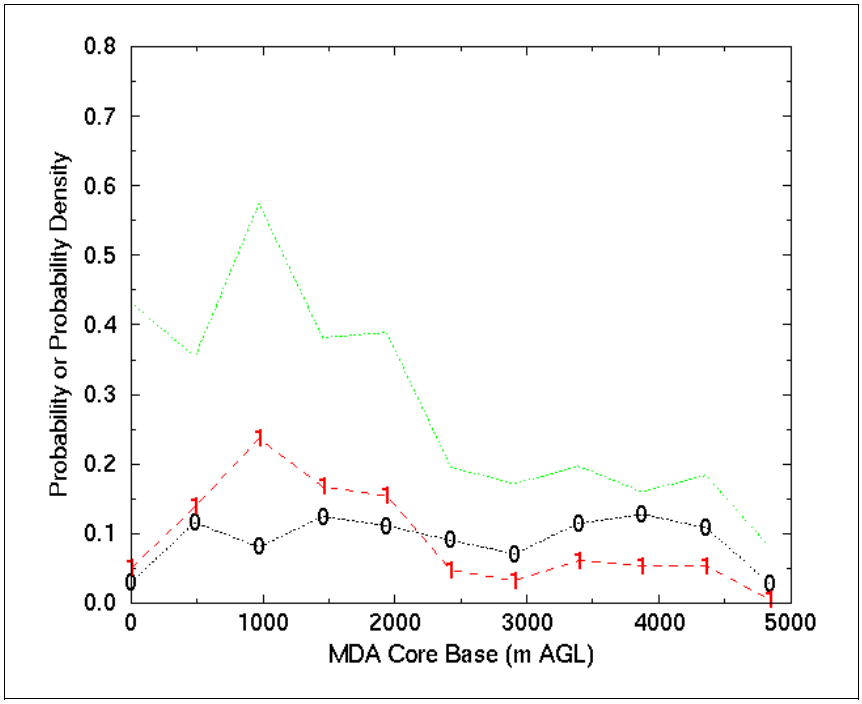

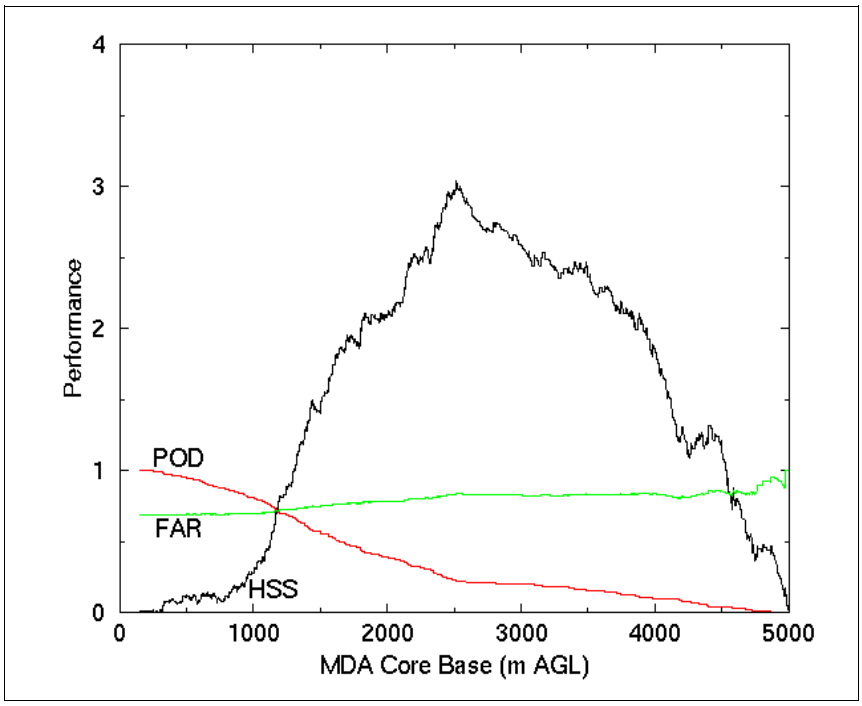

Figure PT-14. TDA low-altitude Gate-to-gate delta-V [LLDV] (m/s): a) Probability plot. In red (solid line) is the probability from Eq. (1) in Appendix B. The dashed (dotted) line with the 1's (0's) is the probability density of tornadic (non-tornadic) detections; b) Decision Threshold plot. POD is in red, FAR is in green, and HSS*10 is in black. For subset III (MDA+TDA) only.

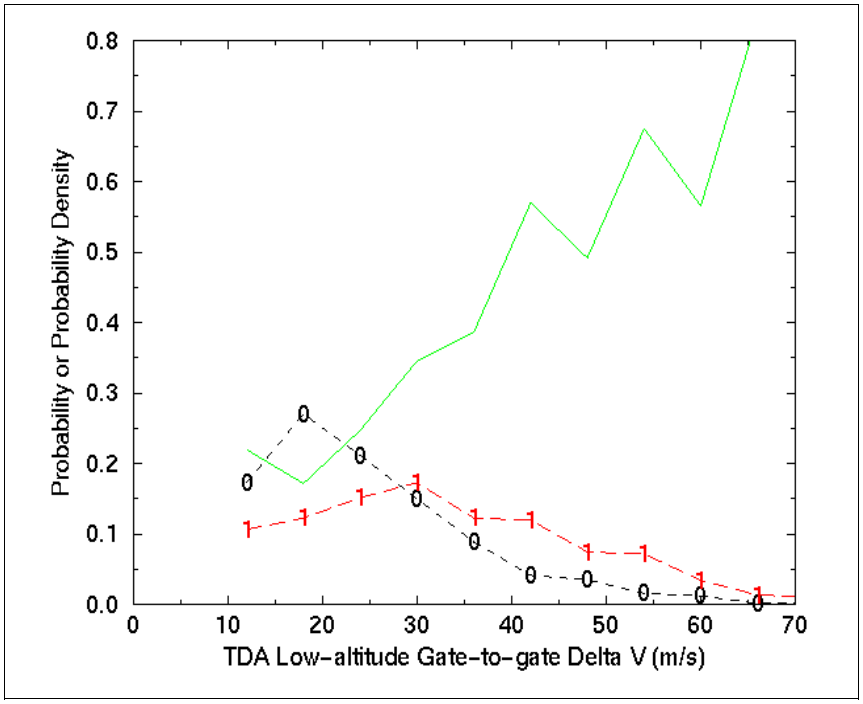

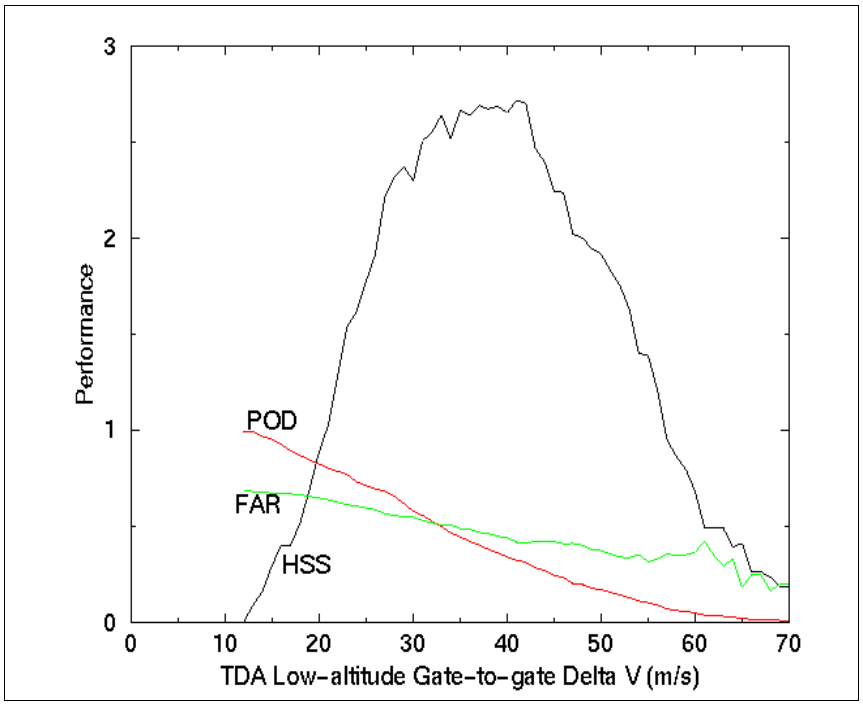

Figure PT-15. TDA maximum gate-to-gate delta-V [MDV] (m/s): a) Probability plot. In red (solid line) is the probability from Eq. (1) in Appendix B. The dashed (dotted) line with the 1's (0's) is the probability density of tornadic (non-tornadic) detections; b) Decision Threshold plot. POD is in red, FAR is in green, and HSS*10 is in black. For subset III (MDA+TDA) only.

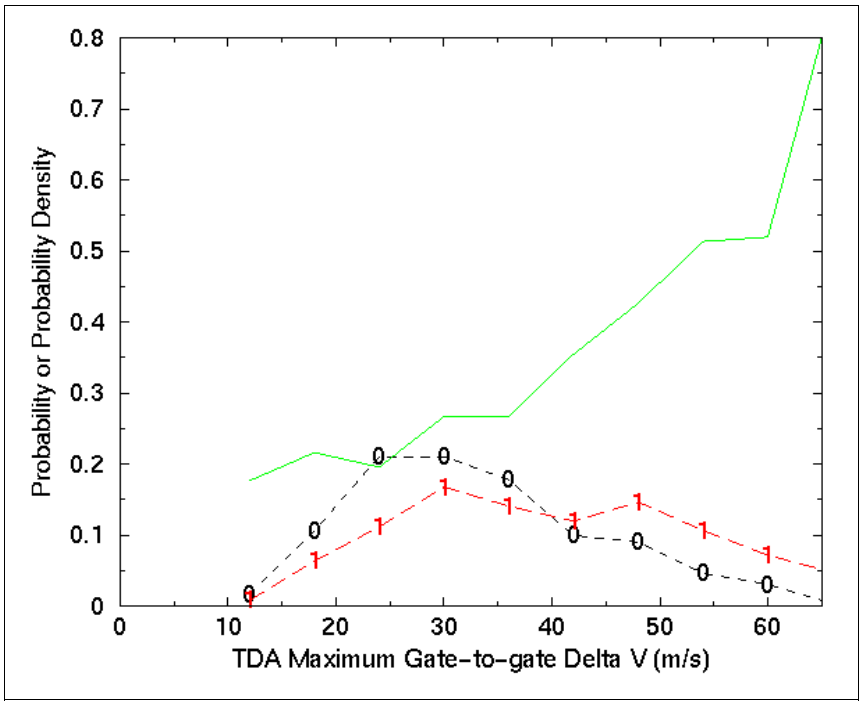

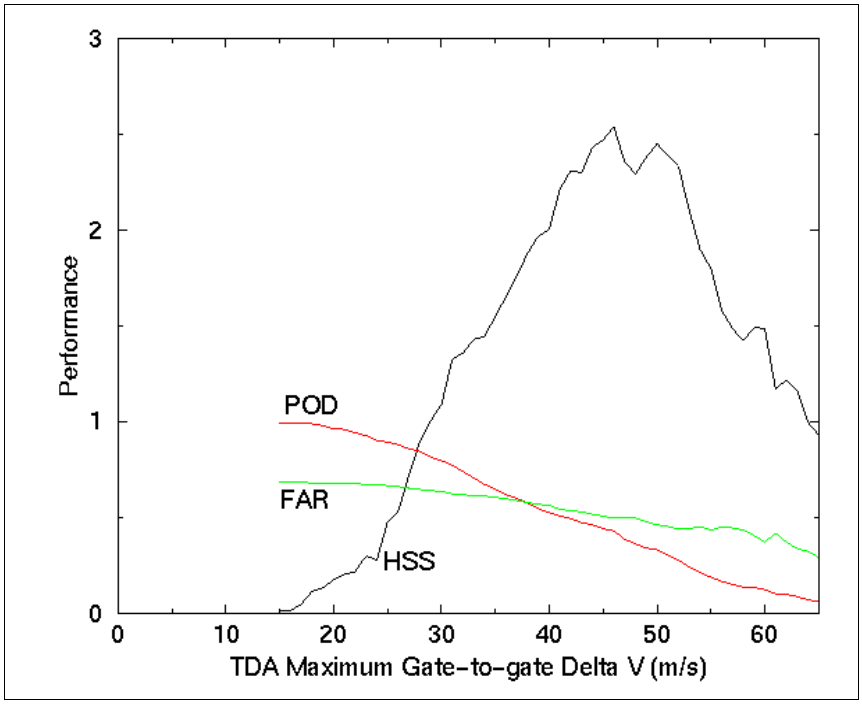

Figure 1. NWS nomogram for mesocyclones with a diameter of 1.0 nm.

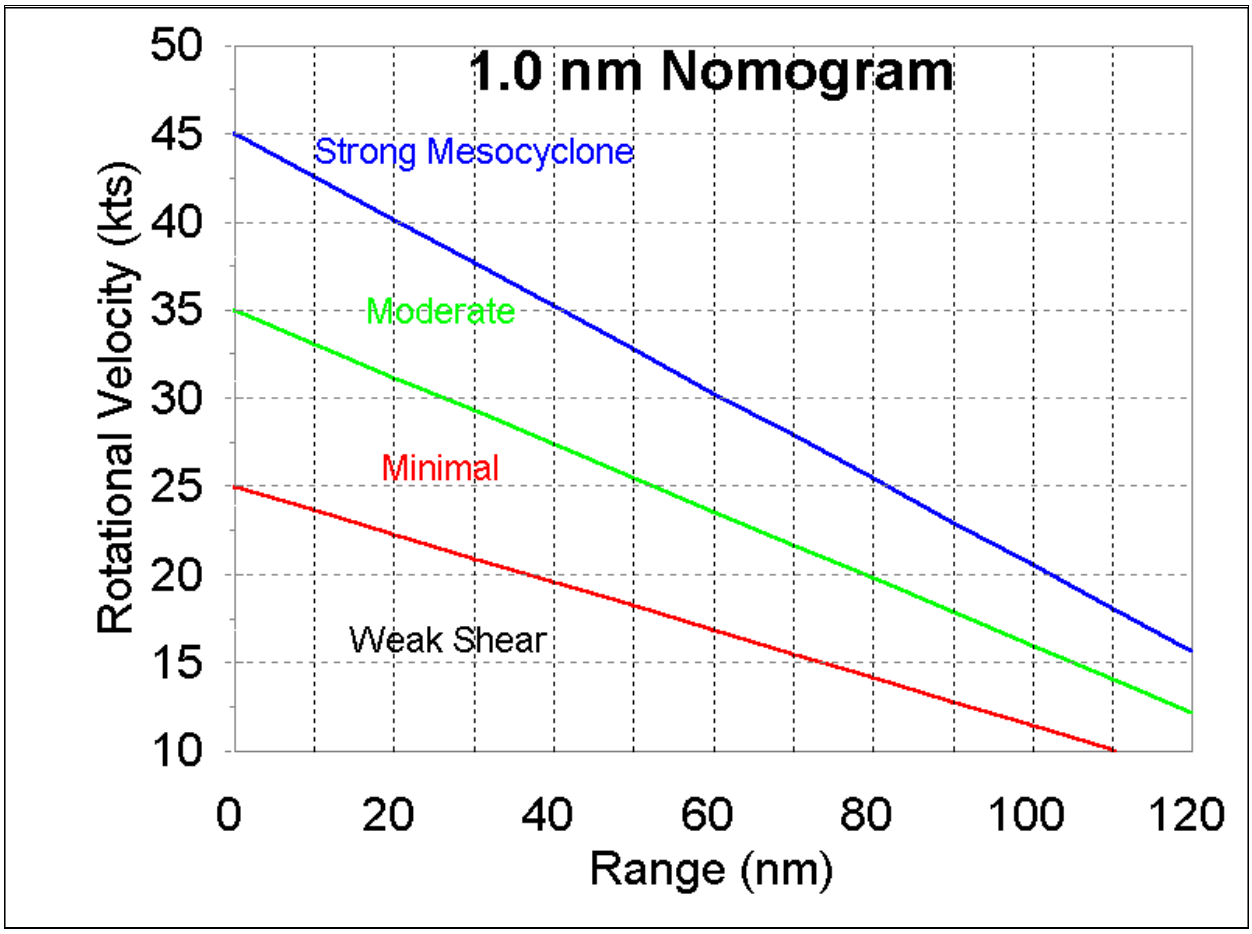

Figure 2. NWS nomogram for mesocyclones with a diameter of 2.0 nm.

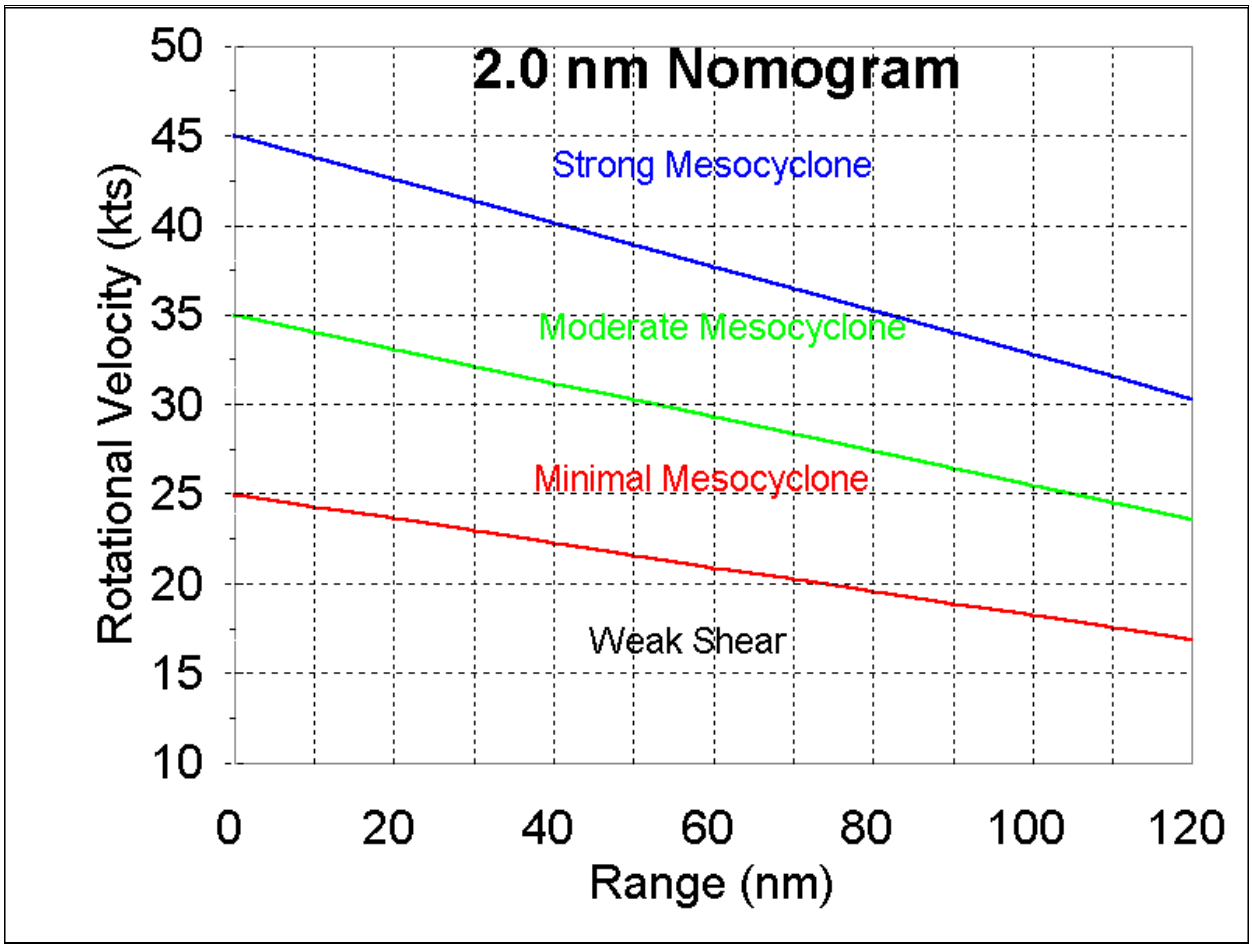

Figure 3. NWS nomogram for mesocyclones with a diameter of 3.5 nm.

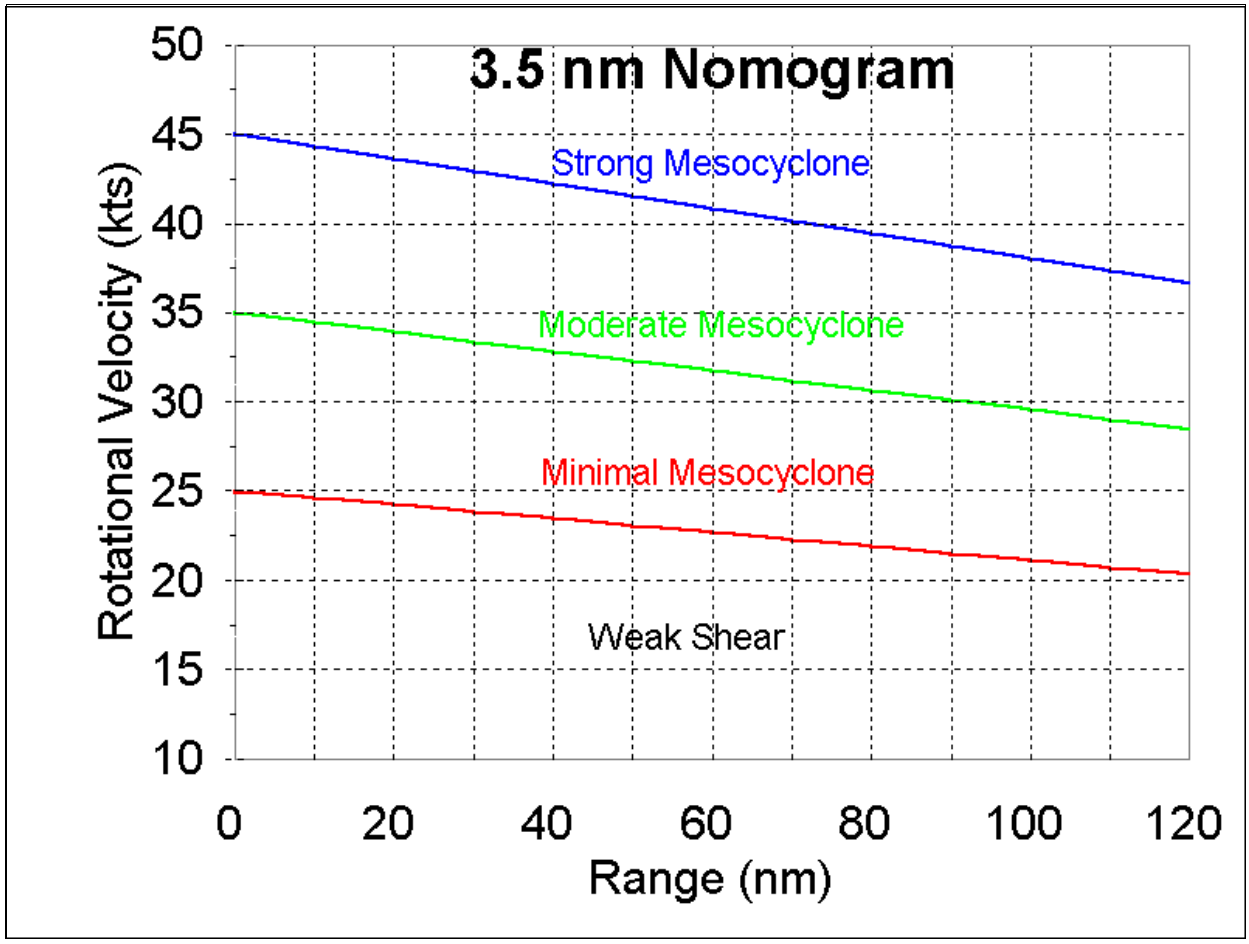

Figure 4. Two examples of a “good” predictor (top and middle), and one example of a “bad” predictor (bottom).

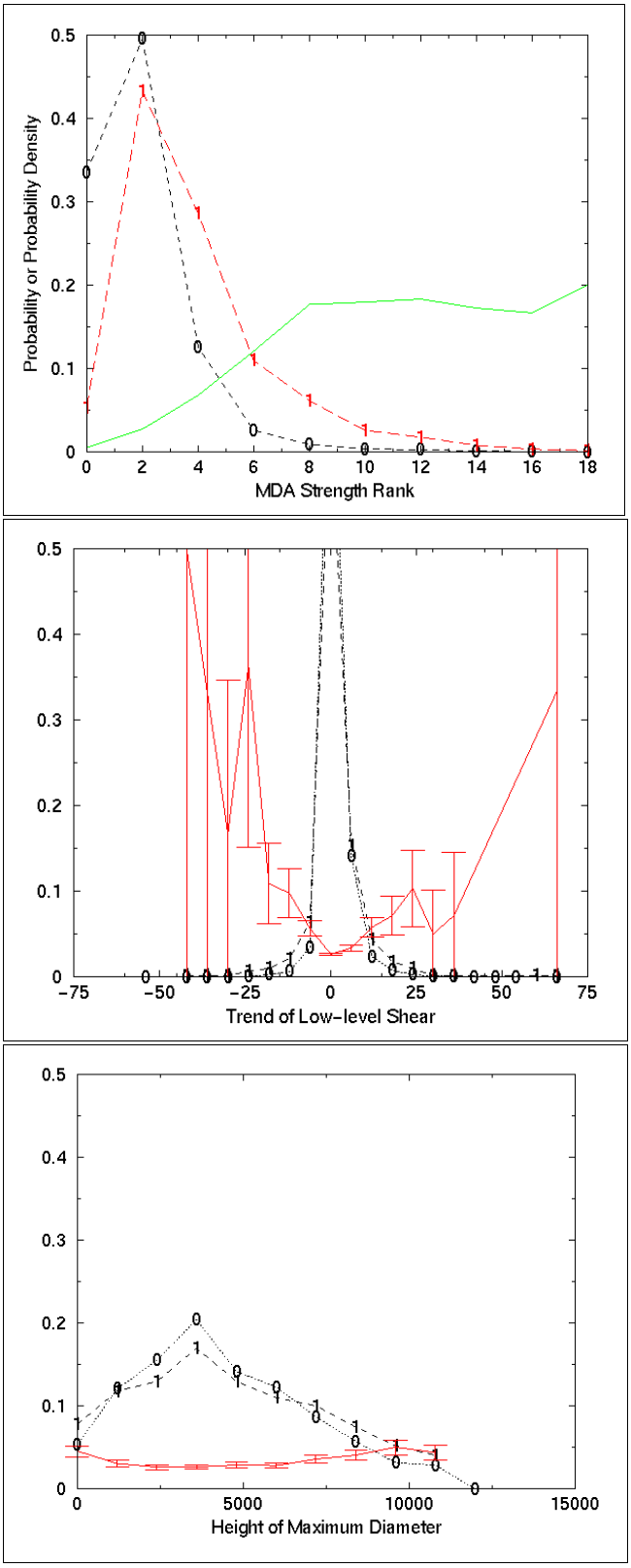

Figure 5. The correlation coefficients between the dependent variable (ground truth) and each of the independent variables for the first three subsets (I, II, and III).

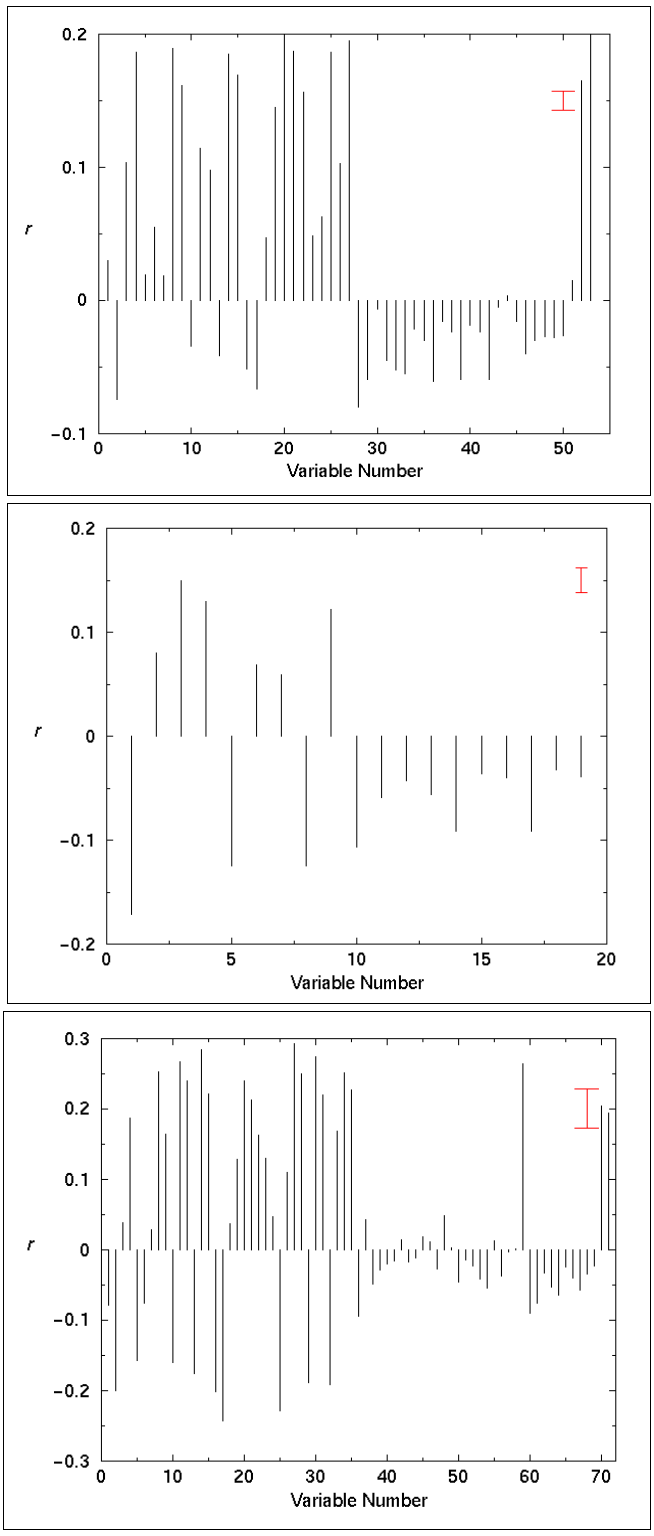

Figure 6. The 53 correlation coefficients in Subset I (i.e. MDA), ordered according to magnitude. 8 variables (in the smaller square) can be identified as the best predictors, and these can be supplemented with another 5 variables (in the larger square).

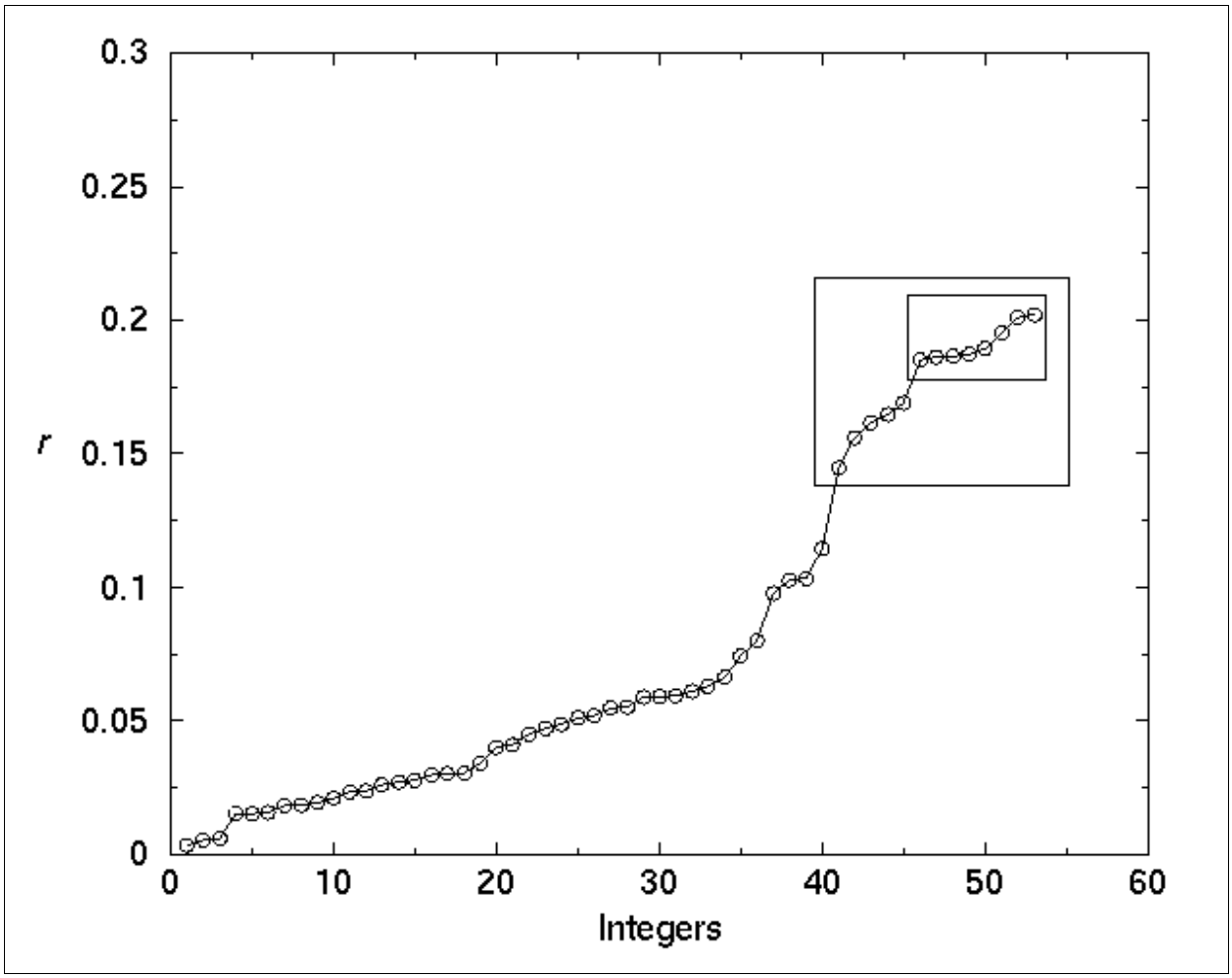

Figure 7. The scatter plot between variables 25 and 53 in subset I (i.e. MDA). The correlation coefficient between the two variables is 0.948, for non-tornadic circulations (black), and 0.950, for tornadic circulations (red).

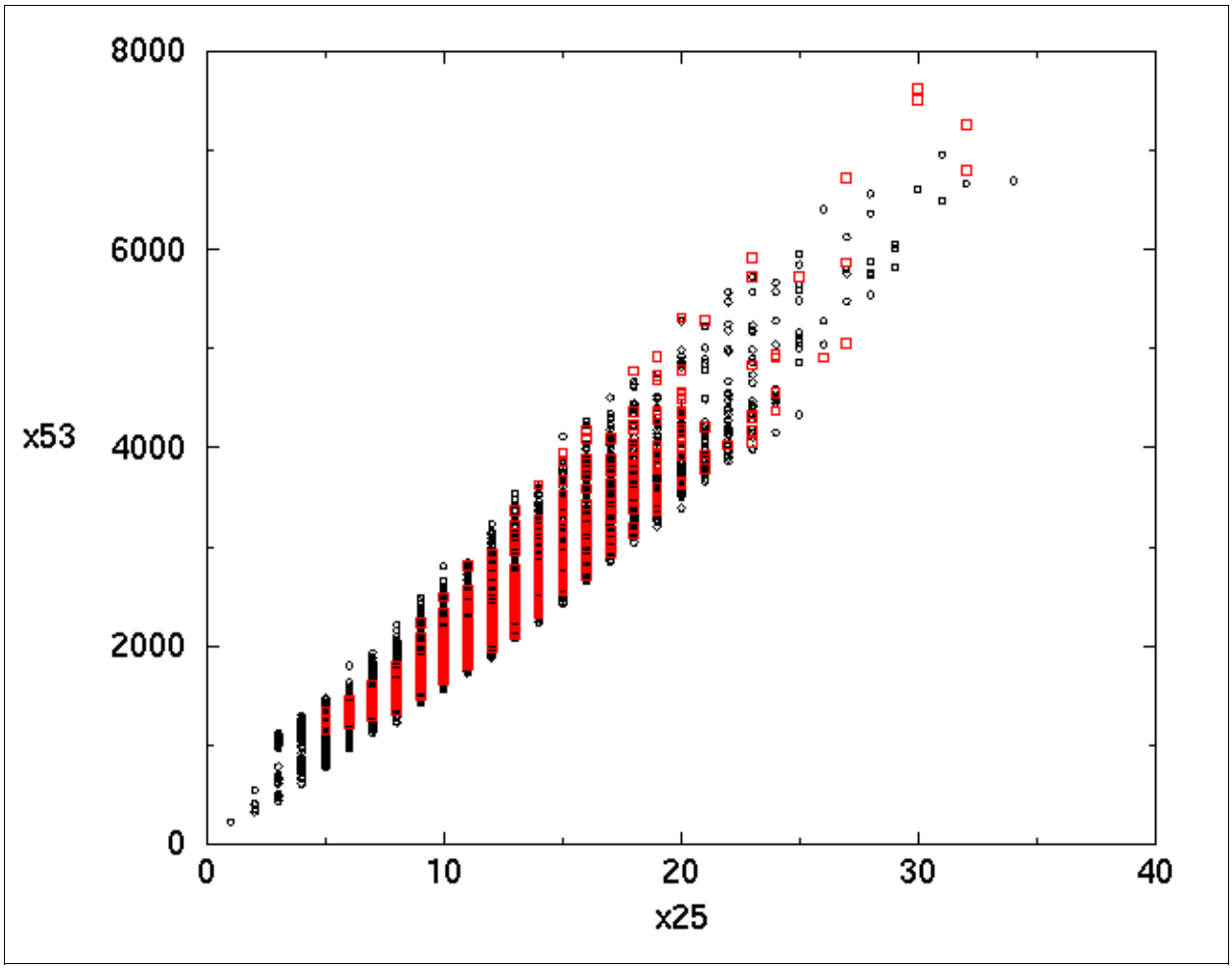

Figure 8. The maximum value of the Critical Success Index (CSI) obtained by dichotomizing the variables in the first three subsets (I, II, and III).

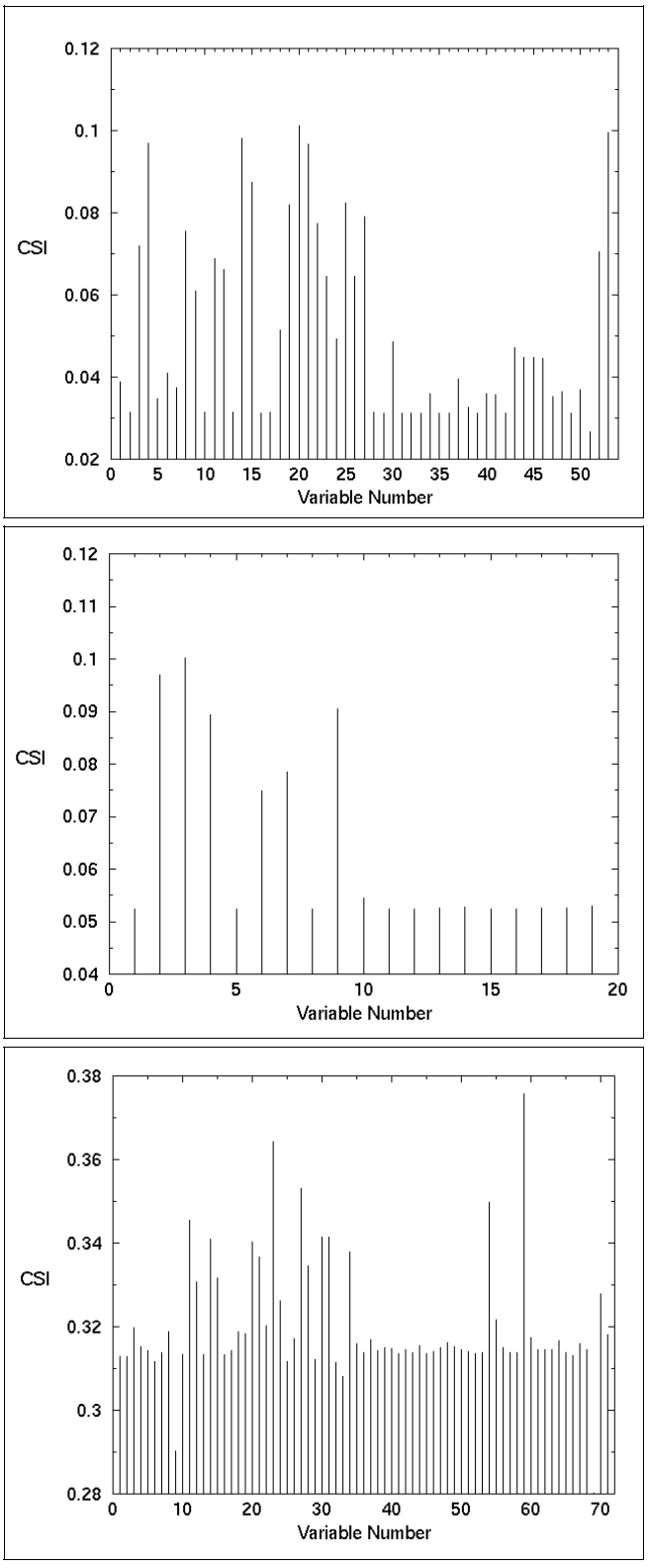

Figure 9. The maximum value of the Heidke Skill Statistic (HSS) obtained by dichotomizing the variables in the first three subsets (I, II, and III).

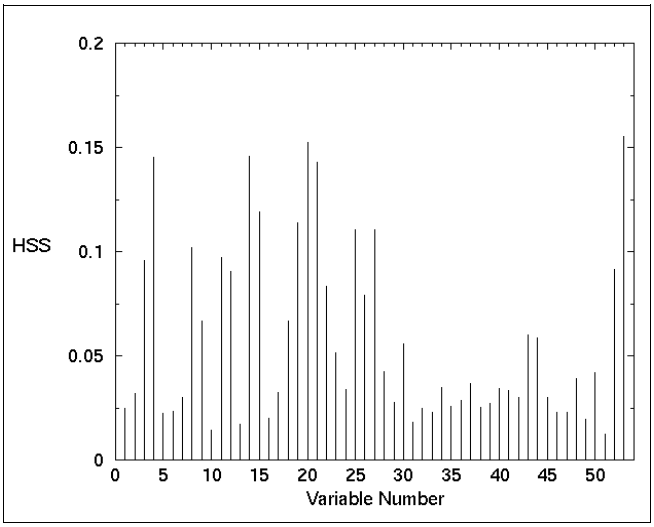

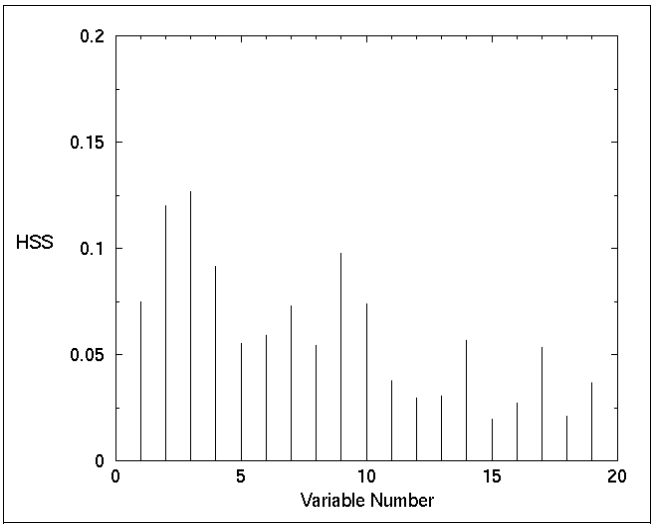

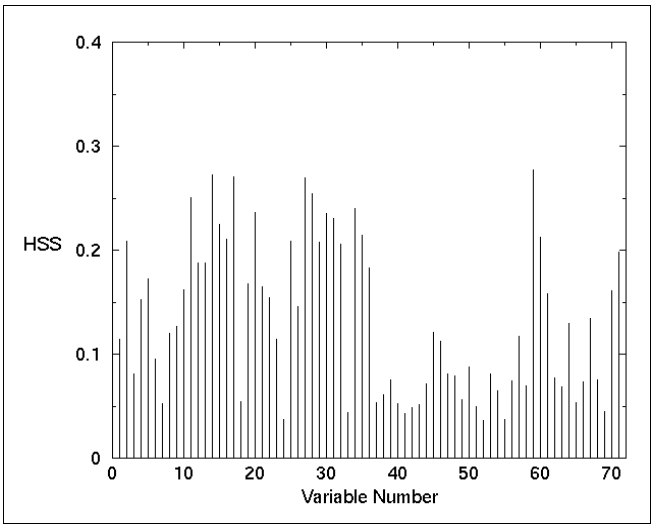

Figure 10. The maximum value of the Entropy (ENT) obtained by dichotomizing the variables in the first three subsets (I, II, and III).

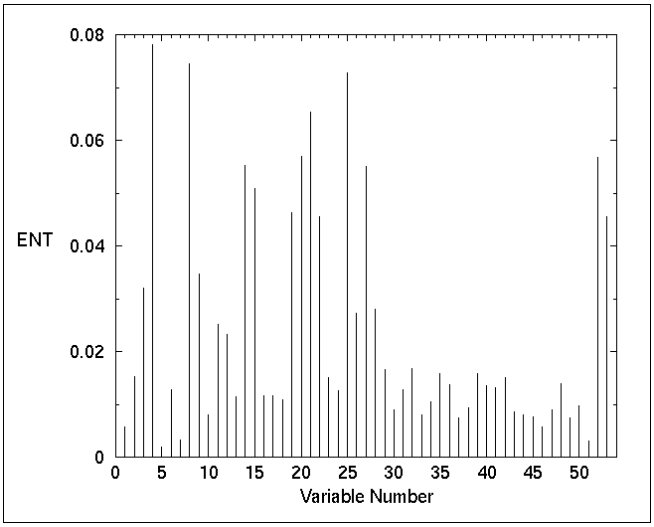

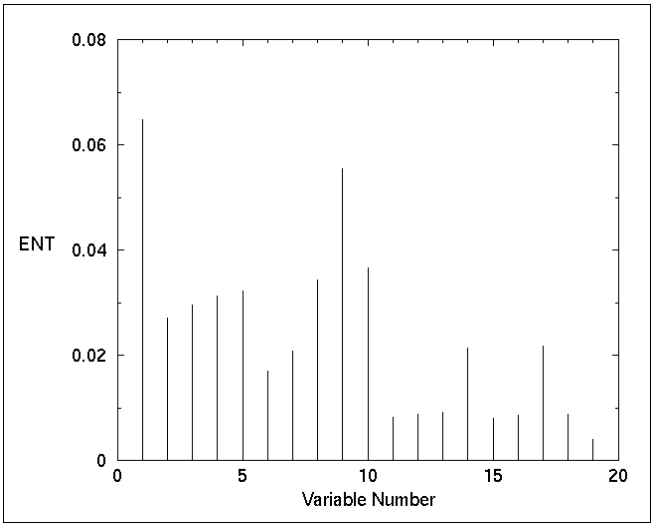

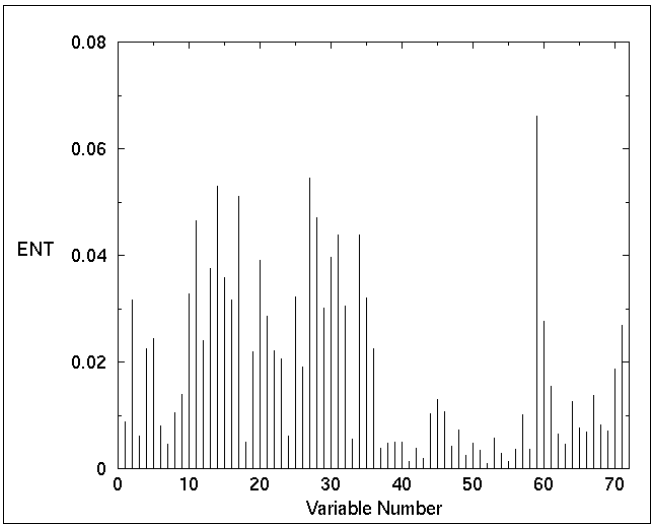

Figure 11. An illustration of the "inequitability" of the CSI. Note that the maximum value of CSI occurs for the smallest value of delta-V.

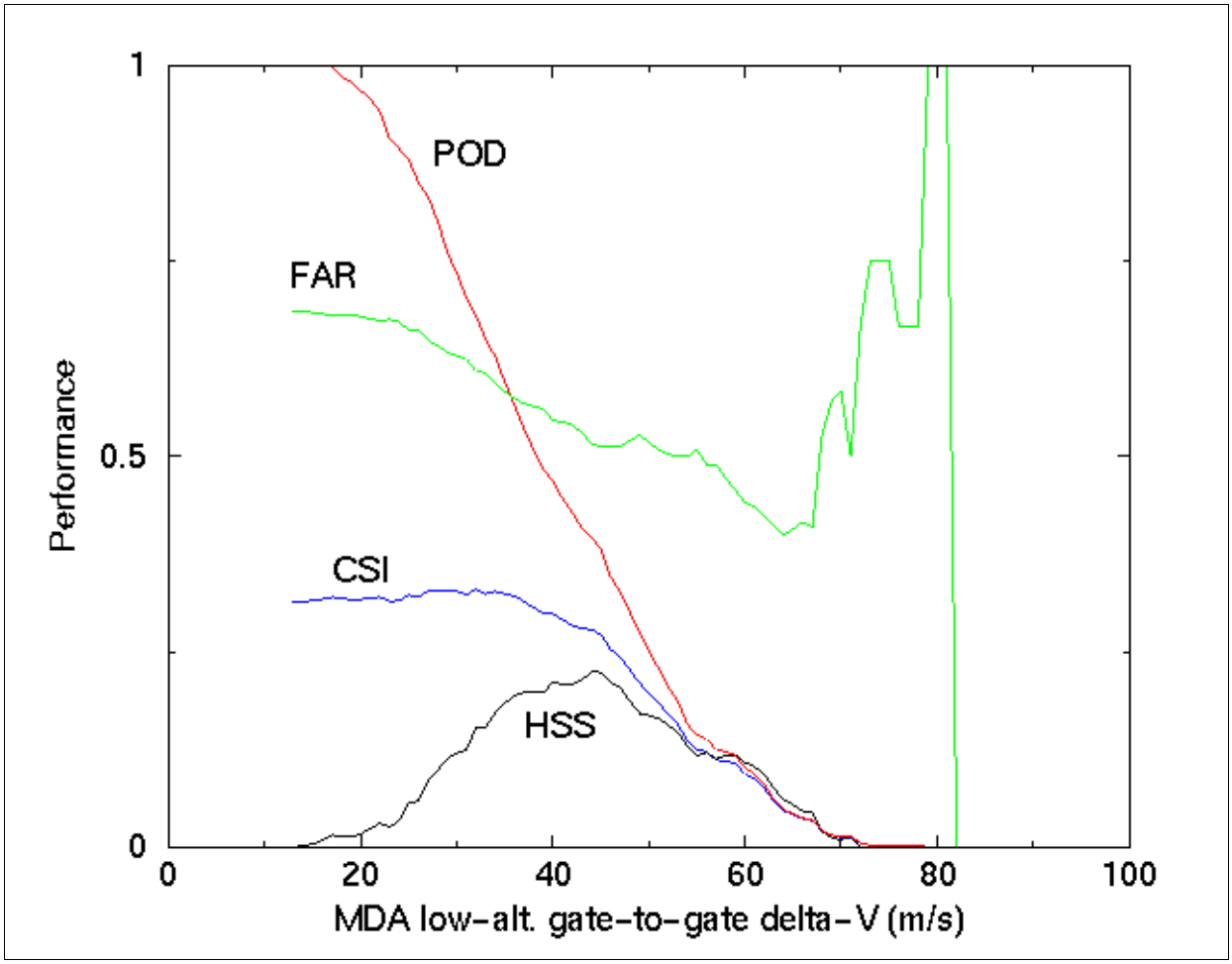

Return to [Top]